NAVAL POSTGRADUATE SCHOOL

MONTEREY, CALIFORNIA

THESIS

LAUNCH PARAMETERS OF AN ICE PAYLOAD TRAVELING VIA LUNAR ELECTROMAGNETIC LAUNCHER TO THE LUNAR GATEWAY

by

Heidi D. Beemer

March 2021

Thesis Advisor: Benjamin T. McGlasson
Co-Advisor: Ian R. McNab

THIS PAGE INTENTIONALLY LEFT BLANK

REPORT DOCUMENTATION PAGE			*Form Approved OMB No. 0704-0188*

1. AGENCY USE ONLY *(Leave blank)*	**2. REPORT DATE** March 2021	**3. REPORT TYPE AND DATES COVERED** Master's thesis

4. TITLE AND SUBTITLE
LAUNCH PARAMETERS OF AN ICE PAYLOAD TRAVELING VIA LUNAR ELECTROMAGNETIC LAUNCHER TO THE LUNAR GATEWAY

5. FUNDING NUMBERS

6. AUTHOR(S) Heidi D. Beemer

7. PERFORMING ORGANIZATION NAME(S) AND ADDRESS(ES)
Naval Postgraduate School
Monterey, CA 93943-5000

8. PERFORMING ORGANIZATION REPORT NUMBER

9. SPONSORING / MONITORING AGENCY NAME(S) AND ADDRESS(ES)
N/A

10. SPONSORING / MONITORING AGENCY REPORT NUMBER

11. SUPPLEMENTARY NOTES The views expressed in this thesis are those of the author and do not reflect the official policy or position of the Department of Defense or the U.S. Government.

12a. DISTRIBUTION / AVAILABILITY STATEMENT
Approved for public release. Distribution is unlimited.

12b. DISTRIBUTION CODE
A

13. ABSTRACT (maximum 200 words)

This paper investigated one possible solution for procuring propellent needed for future space exploration missions. This study examined the feasibility of using an electromagnetic launcher (EML) to transport raw materials used in propellent production from the lunar south pole to NASA's Lunar Gateway. This proposed space station, located in a lunar near-rectilinear halo orbit (NRHO), is a critical part of NASA's Artemis program. Cheaply and efficiently sourcing lunar hydrogen from surface ice to the station would benefit the program's success and future exploration of the solar system. This research investigated the launch requirements for a lunar EML payload. AGI Inc.'s Systems Tool Kit (STK) was used to calculate the required launch azimuth, elevation, magnitude, epoch, and trip duration needed to intercept the Gateway. The model evaluated the payload and the Gateway's radial, cross-track, and in-track positions and rates to determine their relative positions and velocities at rendezvous. Conclusions from this research demonstrated that it is feasible to conduct a single launch from the lunar south pole and target any point along the Gateway's orbit with variable launch conditions. Evidence supporting our hypothesis is presented, showing it may not be possible to match the space station's state vector at rendezvous. The payload will require an additional thrust capability, suggestions for which were also explored in this paper.

14. SUBJECT TERMS NASA, Artemis, Lunar Electromagnetic Launcher, lunar gateway, near-Rectilinear Halo Orbit Lunar South Pole, Systems Tool Kit, launch velocity, Earth-Moon orbital system, LaGrange Point, rendezvous	**15. NUMBER OF PAGES** 85
	16. PRICE CODE

17. SECURITY CLASSIFICATION OF REPORT	**18. SECURITY CLASSIFICATION OF THIS PAGE**	**19. SECURITY CLASSIFICATION OF ABSTRACT**	**20. LIMITATION OF ABSTRACT**
Unclassified	Unclassified	Unclassified	UU

NSN 7540-01-280-5500

Standard Form 298 (Rev. 2-89)
Prescribed by ANSI Std. 239-18

THIS PAGE INTENTIONALLY LEFT BLANK

Approved for public release. Distribution is unlimited.

LAUNCH PARAMETERS OF AN ICE PAYLOAD TRAVELING VIA LUNAR ELECTROMAGNETIC LAUNCHER TO THE LUNAR GATEWAY

Heidi D. Beemer
Captain, United States Army
BS, Virginia Military Institute, 2011
MS, Embry-Riddle Aeronautical University, 2016

Submitted in partial fulfillment of the
requirements for the degree of

MASTER OF SCIENCE IN SPACE SYSTEMS OPERATIONS

from the

NAVAL POSTGRADUATE SCHOOL
March 2021

Approved by: Benjamin T. McGlasson
Advisor

Ian R. McNab
Co-Advisor

James H. Newman
Chair, Space Systems Academic Group

THIS PAGE INTENTIONALLY LEFT BLANK

ABSTRACT

This paper investigated one possible solution for procuring propellent needed for future space exploration missions. This study examined the feasibility of using an electromagnetic launcher (EML) to transport raw materials used in propellent production from the lunar south pole to NASA's Lunar Gateway. This proposed space station, located in a lunar near-rectilinear halo orbit (NRHO), is a critical part of NASA's Artemis program. Cheaply and efficiently sourcing lunar hydrogen from surface ice to the station would benefit the program's success and future exploration of the solar system. This research investigated the launch requirements for a lunar EML payload. AGI Inc.'s Systems Tool Kit (STK) was used to calculate the required launch azimuth, elevation, magnitude, epoch, and trip duration needed to intercept the Gateway. The model evaluated the payload and the Gateway's radial, cross-track, and in-track positions and rates to determine their relative positions and velocities at rendezvous. Conclusions from this research demonstrated that it is feasible to conduct a single launch from the lunar south pole and target any point along the Gateway's orbit with variable launch conditions. Evidence supporting our hypothesis is presented, showing it may not be possible to match the space station's state vector at rendezvous. The payload will require an additional thrust capability, suggestions for which were also explored in this paper.

THIS PAGE INTENTIONALLY LEFT BLANK

TABLE OF CONTENTS

I. INTRODUCTION....1
A. STATEMENT OF PROJECT....1
1. Background....1
2. Objective....1
3. Methodology....2
4. Analysis and Results....2
B. PROBLEM IDENTIFICATION....2
1. Hypothesis....2
2. Subsidiary Research Questions....3

II. REVIEW OF RELEVANT LITERATURE....5
A. HISTORY OF SPACE EXPLORATION....5
1. Refueling in Space....6
2. Lunar Resources....6
3. Transporting Ice into Lunar Orbit....8
B. ELECTROMAGNETIC LAUNCHER USE IN SPACE APPLICATIONS....9
1. History of Earth-Based Electromagnetic Launch....9
2. History of NASA Research in Lunar-Based Electromagnetic Launch....11
3. Proposed Electromagnetic Launcher Designs....12
C. ARTEMIS....15
1. Artemis Accords....16
2. Lunar Gateway....16

III. METHODOLOGY AND MODEL DESIGN....21
A. DESIGN....21
1. Components....21
2. Reference Frame....29
3. Perturbations....29
B. DATA ANALYSIS....29
C. ASSUMPTIONS....30

IV. RESULTS....31
A. LOCATING THE GATEWAY....31
B. DIFFERENTIAL CORRECTOR....34
C. LAUNCH EPOCH....40

D. LAUNCH DURATION 40
E. TARGETING GATEWAY RIC FOR ZERO RELATIVE VELOCITY 42
F. OTHER SCENARIOS TESTED 43
1. Scenario 1 44
2. Scenario 2 45
G. ACHIEVING RENDEZVOUS WITH THRUSTERS 45

V. CONCLUSION AND RECOMMENDATIONS 51
A. CONCLUSIONS 51
1. Support for the Hypothesis 51
2. Optimal Launch Parameters 52
3. Conclusions from Other Launch Scenarios 53
B. RECOMMENDATIONS 54
1. Thruster Parameters 54
2. Commercial-Off-the-Shelf Thrusters 59
C. FUTURE RESEARCH 60

LIST OF REFERENCES 63

INITIAL DISTRIBUTION LIST 67

LIST OF FIGURES

Figure 1. Lunar Oxygen Delivery Orbits and Missions. Source: Snow and Kolm (1992). 8

Figure 2. Concept Drawing for a Hypersonic Flight System Launched from EML Track at Kennedy Space Center. Source: Starr (2010). 11

Figure 3. Rail Gun Model. Source: Stewart (2016). 13

Figure 4. Design for a Coilgun Varient Known as Quenchgun Source: Nottke and Bilby (1990). 15

Figure 5. Lunar Gateway Concept Art. Source: NASA (2020a). 17

Figure 6. Halo Orbit Families in the Earth-Moon System. Source: Lee (2019). 18

Figure 7. The Initial State of the Target Sequence 23

Figure 8. Spacecraft Parameters for the Payload 24

Figure 9. Example Transfer Orbit Targeting the Gateway. Adapted from Sellers et al. (2000). 25

Figure 10. Maneuver Segment of the Target Sequence 26

Figure 11. Propagate Segment of the Target Sequence 27

Figure 12. STK Model of NRHO Earth-Centered Reference Trajectory 28

Figure 13. STK Model of NRHO Moon-Centered Reference Trajectory 28

Figure 14. 3D Visualization of Close Approach Between Gateway and Payload Near 90° Azimuth 33

Figure 15. Maneuver Segment Thrust Vector Used to Target Position 3 33

Figure 16. Selected Results for Propagate Segment 34

Figure 17. Differential Corrector for Target Sequence 35

Figure 18. EML Thrust Vector Calculated by the Target Sequence 35

Figure 19. 3D Rendering of the 43 iterations Calculated by the Target Sequence. 36

Figure 20. Target 1 at Point of Rendezvous 38

Figure 21. Target 2 at Point of Rendezvous 38
Figure 22. Target 3 at Point of Rendezvous 39
Figure 23. Target 4 at Point of Rendezvous 39
Figure 24. Adding Rates as Results Within the Propagate Segment 43
Figure 25. Second Target Sequence added to the Mission Control Sequence 46
Figure 26. Target Sequence Results for a Chemical Engine 47
Figure 27. 3D Graphics at the Point of Intercept Using a Chemical Engine 47
Figure 28. Target Sequence Results for a Cold Gas Engine 48
Figure 29. 3D Graphics at the Point of Intercept Using a Cold Gas Engine 49
Figure 30. Exhaust Velocities as a Function of Typical Vehicle Accelerations. Source: Sutton and Biblarz, (2017). 56

LIST OF TABLES

Table 1. Moon AER Data and calculated Payload Time of Flight.....32

Table 2. Thrust Vector Results and Gateway RIC at Rendezvous 37

Table 3. Fixed Velocity at Time of Rendezvous 37

Table 4. Range of Launch Epochs Between Lunar Equatorial Plane at Apolune.....41

Table 5. Results of Differential Corrector Targeting Gateway RIC and Trip Duration of Trial 3 41

Table 6. RIC Rates for the Gateway and Payload at 6 Jan 2022 07:58:15.630 42

Table 7. Scenario 1 Launch Parameters.....45

Table 8. Scenario 2 Launch Parameters.....45

Table 9. The Difference in Fixed Velocity at Intercept with Chemical Engine 47

Table 10. The Difference in Fixed Velocity at Intercept with Cold Gas Engine.....48

Table 11. Optimal Position 52

Table 12. Required Maneuver by Payload Engine 55

Table 13. Overview of Common Application for Different Propulsion Systems. Source: Wertz et al., (2011).....56

THIS PAGE INTENTIONALLY LEFT BLANK

LIST OF ACRONYMS AND ABBREVIATIONS

ASTP	Advanced Space Transportation Program
DRO	distant retrograde orbits
EM	electromagnetic
EML	electromagnetic launcher
ESR&T	exploration systems research and technology
GPHS-RTG	general purpose heat source-radioisotope-fueled thermoelectric generators
H2	hydrogen molecule
H2O	water molecule
HALO	Habitation and Logistics Outpost
HPOP	High-Precision Orbit Propagator
ISP	specific impulse
ISRU	in situ resource utilization
kg	kilogram
km	kilometer
L1	first Lagrange point
L2	second Lagrange point
LEML	lunar electromagnetic launch systems
LEO	low Earth orbit
LH2	liquid hydrogen molecule
LLO	low Lunar orbits
LSR	lunar synodic resonance
MagLev	magnetic levitation
MIT	Massachusetts Institute of Technology
NASA	National Aeronautics and Space Administration
NRHO	near-rectilinear halo orbit
O2	oxygen molecule
PPE	power and propulsion element
RIC	radial, in-track and cross-track
SLS	space launch system
STK	system tool kit
t	metric ton
TOF	time of flight

THIS PAGE INTENTIONALLY LEFT BLANK

ACKNOWLEDGMENTS

I want to thank my advisors, Dr. Ian R. McNab and Dr. Ben T. McGlasson, for their mentorship during my thesis. It has been exhilarating for me to express my passion for human space exploration in the form of a project that may one day impact future missions. It was a unique experience working long distance with an advisor that lived 15 miles from my wife in Austin, Texas, while I worked remotely 1,446 miles away at NPS. I look forward to meeting in person soon. post-pandemic. I would also like to thank LTC Craig Boucher for his assistance and guidance regarding my model and using STK. A special thank you to Liam Robertson for providing quick and timely assistance from AGI support. The true hero of my second master's experience was Dr. Wenschel Lan, who proved an excellent sounding board and mentor who got me through all that was the 2020–2021 academic school year. I appreciate your advice and support.

I want to thank Col John Hartke, the House of PANE Department Head at West Point, for believing I would make a valuable part of his West Point team. I would also like to thank COL Peter Chapman, the PANE Deputy Department Head, for not giving up on me and insisting that I apply to the Naval Postgraduate School. I am excited to join the team in the next few months, and this degree would not have been a reality without your support.

Above all, I would also like to thank my wife, Sofia, for her continuous encouragement. In my first master's thesis, I referred to her as my favorite rock, a pun that played well with the topic of study. Here, I think she could better be described as a boulder. Strong and determined to make things work long distance over 18 trying months, thousands of miles apart, all while a global pandemic raged on, to allow me to pursue an opportunity to further my education and career. I am forever grateful for your love and support, and I am excited about our next chapter together at West Point.

THIS PAGE INTENTIONALLY LEFT BLANK

I. INTRODUCTION

A. STATEMENT OF PROJECT

1. Background

Humanity aspires to become a multi-planetary species. However, many difficult questions must be addressed to accomplish this. The United States' scientific community has long debated whether the Moon or Mars should be the first permanent, off-planet destination. Both locations have their pros and cons, but the Moon's resources have the potential to drastically reduce the cost of reaching farther destinations.

It is well established that there is accessible water, in the form of ice, on the Moon's surface (Honniball et al., 2020). Suppose a means of cheaply and efficiently transporting this ice from the surface into space is developed. In that case, these raw materials can be manufactured on orbit into highly efficient fuel used as a propellant for interplanetary spacecraft. Why continue to rely solely on traditional chemical rockets using propellent to transport propellent? The Moon should be leveraged for these resources, and alternative launch technologies should be developed to create a sustainable spacefaring architecture to explore the solar system further. These topics are investigated within this thesis, and a recommendation for the use of electromagnetic launchers (EML) is made.

2. Objective

The efforts produced by this thesis will contribute to the National Aeronautics and Space Administration's (NASA) ability to transport mined lunar ice found in the southern craters on the Moon's surface to an intermediate space station, called the Gateway, located in the Earth-Moon orbital system. It is expected that this research will assist NASA in determining the validity of using a lunar EML (LEML) to transport this payload from the surface. Precisely, it evaluates the launch angle and velocity required to leave the Moon's surface and intersect with the Gateway. This study is being conducted in conjunction with scientists and engineers from NASA Armstrong (Edwards AF Base), currently analyzing the ability to support human space exploration missions to the Moon by 2024 and future potential for further deep-space exploration.

3. Methodology

This thesis aims to develop a model of an EML on the lunar surface's south pole to NASA's Gateway using computer simulation software. The parameters for this launch, including angle and velocity, will be investigated and modeled. Suppose it is determined that the payload cannot feasibly arrive at the Gateway at relative rest. In that case, an investigation into thruster requirements will be included in the research.

4. Analysis and Results

Reports and 3D graphics generated by simulation software, such as azimuth, elevation, range (AER), the Mission Control Sequence (MCS) summary, and radial, in-track, cross-track (RIC) will be generated. The data will be analyzed to determine the position and velocity of a launched lunar payload with respect to the lunar Gateway, varying along its orbital path.

B. PROBLEM IDENTIFICATION

This study identifies the launch parameters required for an EML located on the south pole of the Moon to launch a self-contained payload, containing either raw ice or liquid hydrogen (LH_2), from the surface to intercept with the Gateway space station, located within a near-rectilinear halo orbit, and arrive at a velocity matching the relative speed of the station.

1. Hypothesis

Previous research conducted by Ian McNab suggests that a change in velocity (ΔV) of 2.8 km/s will be required to launch a payload containing raw propellent from the lunar south pole to rendezvous with the Moon-Earth L2 Lagrange point (I. McNab, email to author, August 12, 2020). It is hypothesized that the payload will intercept the Gateway with an initial velocity less than 2.8 km/s at several points along the spacecraft's trajectory but will not achieve a terminal velocity near rest, requiring further modifications to the payload to account for additional flight hardware.

a. Independent Variables

The variables tested through modeling software will be azimuth, elevation, magnitude, the payload's orbit epoch, and trip duration.

b. Dependent Variables

The variable that will depend on this study's independent variables will be the position and velocity vectors of the lunar payload and the Gateway during rendezvous.

c. Interpretation of Findings

Based on the model results, data will be reviewed and presented using visual means such as models, and tables. The findings will be interpreted from this data to determine if the payload can feasibly intercept the Gateway's orbit at a near-zero relative velocity. Subsidiary research questions will need to be addressed if the payload does not match its target's relative velocity.

2. Subsidiary Research Questions

Supporting questions developed for this research pertain to the Gateway payload. If the speed at intercept is too great, it will be determined that onboard thrusters will be required to reduce or increase the capsule's velocity to match that of the space station. The questions are, therefore:

1. Will terminal guidance thrusters be required to achieve a terminal velocity matching the Gateway?
2. What are the parameters of these thrusters?
3. What commercial-off-the-shelf thrusters exist that would meet the required parameters?

THIS PAGE INTENTIONALLY LEFT BLANK

II. REVIEW OF RELEVANT LITERATURE

A. HISTORY OF SPACE EXPLORATION

Human space exploration is challenging, as dozens of problems must be addressed before achieving an established human presence on any planet or moon within the solar system: everything from essential life-support systems, communication capabilities, radiation shielding, and the ability to land these systems on the surface of moons and planets, with varying atmospheres and gravity requirements (Beemer & Worrells, 2017). Despite these apparent challenges, since the 1972 Apollo Moon missions, the last three presidents of the United States have outlined specific plans to develop and test imperative space architecture needed to further human exploration of space (National Aeronautics and Space Administration [NASA], 2004).

For example, the United States has long since debated the importance of using the Moon as a launch point for further space exploration missions. In 2004, President George W. Bush established the Moon as "an important step for [his] space program" in a speech made to the National Air and Space Administration announcing the launch of the President's vision for space exploration (Office of the Press Secretary, 2004, para. 17). In this speech, the President outlined the advantages of using the Moon as the first step before sending human missions to Mars and beyond. He reasoned that an "extended human presence on the moon" would significantly reduce cost and risk for future missions (Office of the Press Secretary, 2004, para. 12). The President also explicitly referenced fuel concerns, declaring that while launching these resources from Earth was expensive, it would be possible to harvest and launch raw materials from the Moon's surface to be "processed into rocket fuel and breathable air" (Office of the Press Secretary, 2004, para. 17).

The idea of harnessing rocket fuel from the moon has not come to fruition, however, developments like SpaceX reusable rocket technology has significantly lowered the price per launch kilogram (kg). In general, commercial rockets have reduced the cost of getting to LEO from $5,200 per kg using Saturn V hardware to $1,410 per kg with SpaceX's

Falcon Heavy (Jones, 2018). As revealed by David Chato in a NASA technical memorandum, launch costs are calculated based on the destination. In his research, Chato discusses how the cost of getting into high earth orbit, lunar orbit, or Martian orbit only increases as more stages and fuel are required. Currently, space launch requires that storage containment components be relaunched, adding additional weight and cost to each mission. The additional cost of launching storage tanks, equipment, and fuel each time would be a waste of weight and drive the mission's cost beyond what is financially feasible and sustainable. A crucial step for any human space exploration mission beyond the Moon will be designing the technology required to store fuel and the equipment needed to refuel spacecraft in orbit (Chato, 2005).

1. Refueling in Space

One of the most "difficult technology challenges," according to Paul Wooster, SpaceX's principal engineer of the Starship project, is the ability to refuel on-orbit (Berger, 2019, para. 4). Space refueling is a topic that engineers have studied for decades. NASA's Exploration Systems Research and Technology (ESR&T) program at the Glenn Research Center, Cleveland, Ohio, was tasked with exploring this problem set and has highlighted several concerns with the existing technology. Current research has been theoretical and challenging to test on-orbit without launching experiments specifically designed to test how an open system would react in the environment of space. The scientific community agrees that new technology is needed and must be proven on-orbit to thoroughly test the concept of maintaining propellant storage tanks in space, including long-term storage, pressure control, mass gauging, and liquid acquisition (Chato, 2005).

2. Lunar Resources

In Situ Resource Utilization (ISRU) is NASA's use of indigenous resources found on other moons and planets to sustain colonists during extended-duration missions. Referred to as living "off the land," NASA defines IRSU as "any hardware or operation that harnesses and utilizes in-situ resources to create products and services for robotic and human exploration" (Green & Kleinhenz, 2019, p. 2). This concept is an essential part of any long-duration mission proposal and has been researched by NASA's human space

exploration community for decades (Wright et al., 2011). Leveraging local resources lowers the overall mission's cost and complexity, increases sustainability, reduces mission and crew risk, and increases its ability to complete science objectives. NASA considers ISRU to be an implied requirement for all future human-crewed missions (Green & Kleinhenz, 2019).

Ice plays a critical role in the ISRU conceptual plan for lunar colonization, as a lunar colony would harvest ice for drinking, shielding from radiation, growing food, and crew hygiene. Settlers would also use harvested ice for its essential hydrogen (H_2) and oxygen (O_2) components. Oxygen molecules would be used for breathing and oxidizer for propulsion and power, while hydrogen could be used as rocket propellent (Green & Kleinhenz, 2019). Luckily, the scientific community continues to find this valuable resource locked in the lunar regolith covering the Moon's surface. Instrumentation, such as the Lunar Prospector neutron spectrometer of the Los Alamos National Laboratory, have mapped hydrogen concentration of the lunar north and south poles and have located approximately three billion metric tons (t) of water ice (Siegfried, 2000). In 2008, NASA's Lunar Crater Observation and Sensing Satellite (LCROSS) intentionally crashed into the lunar south pole to observe the ice ejecta cloud that resulted from impact (Noneman, 2007). Current research postulates that the ice exists in small grains less than 10 cm in size and mixed into the lunar regolith. Scientists at NASA also suggest that thin coatings of ice may exist on rocks within these craters (Anand et al., 2012). Most studies have focused on the poles where craters remain shielded from the sun; however, recent evidence has shown that lunar craters on the sun-light side of the Moon also harbor ice, although in lesser concentrations as a function of latitude (Honniball et al., 2020).

Although lunar ice will be mined using mostly remote technology, colonists stationed on the Moon will supervise the activity and equipment maintenance (Siegfried, 2000). Extracting ice from dark, cold environments at the poles will be a challenge, and understanding the nature of this ice will be essential in extracting it for further use. NASA engineers and scientists have researched several harvesting methods for acquiring raw lunar ice. These methods include the use of microwave heating, general-purpose heat source-radioisotope-fueled thermoelectric generators (GPHS-RTG), or solar thermal

processing (Siegfried, 2000). NASA has also proposed using hydrogen reduction to harvest resources (Green & Kleinhenz, 2019). Lunar mining will provide colonists with the resources they need to continue their mission on the Moon and beyond and simultaneously have scientific significance by adding to the current knowledge regarding lunar geology and structure of the Moon (Fields et al.,1967).

3. Transporting Ice into Lunar Orbit

As early as 1950, scientists explored the feasibility of transporting raw materials for making fuel from the Earth's surface into earth-orbit (Clark, 1950). Over time, the concept was expanded to apply to transporting materials from the lunar surface into lunar and then Earth orbit, as seen in Figure 1. Fuel harvested from the Moon's surface will likely be considered a valuable and finite resource. According to W. Siegfried, lunar colonies will be consuming 10 t per year of O^2 and 300 t per year of $H^{2,}$ requiring over 700 t per year of lunar regolith to be processed (Siegfried, 2000). Currently, new remote sensing experiments have a better understanding of the overall hydration on the lunar surface. However, estimates for the total amount of ice can only be extrapolated due to limited observation of the dark side of the Moon.

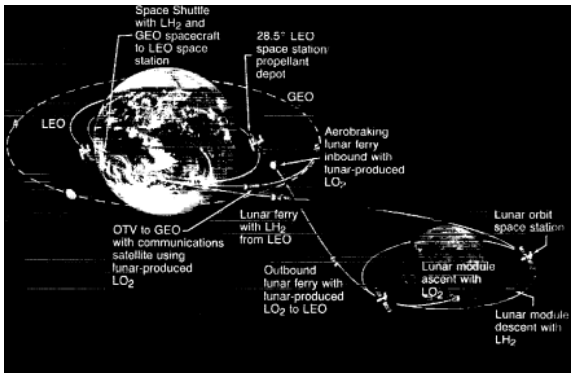

Figure 1. Lunar Oxygen Delivery Orbits and Missions.
Source: Snow and Kolm (1992).

Once fuel is harvested, however, the launch vehicle used to transport this payload into space must overcome the Moon's escape velocity. If the launch velocity is not equal

to this limiting speed, then the object launched will fall back to the surface of the Moon. Escape velocity for the moon would be 2375.89 m/s as calculated by:

$$V_{esc} = \sqrt{\frac{(2GM)}{r}}, \tag{1}$$

where:

G= Gravitational Constant of the Moon (Nm/Kg^2)
M= Mass of the Moon (kg)
r= Radius of the Moon (m).

Therefore, any payload launched from the surface must be launched at a velocity greater than or equal to 2.38 km/s.

Further, using raw lunar ice as a chemical fuel to transport chemical propellants is counterproductive. Research into alternative launch technologies has long been a focus for NASA; methods that can be powered using natural power sources, such as solar or nuclear, would be ideal for this refueling problem. In addition, EML designs have been conceptualized for Earth and the Moon in many projects, and electromagnetic launch capabilities would provide an alternative to chemical-based launch machines and could be an effective means of transporting the Moon's surface materials.

B. ELECTROMAGNETIC LAUNCHER USE IN SPACE APPLICATIONS

Transporting lunar harvested liquid H_2 or solid H_2O for fuel using EML systems have been widely researched over the last century. This technology would turn stored energy into a propulsive force capable of launching these raw materials into space for storage and later use. According to an article published in the *IEEE Transactions on Plasma Science*, the authors support the notion that EML would be a more cost-effective, safest, and most efficient means of transporting critical materials from lunar depots. (Wright et al., 2011).

1. History of Earth-Based Electromagnetic Launch

As stated in William Snow and Henry H. Kolm's 1992 paper, EMLs have been designed and tested as a terrestrial weapon system since 1901. Issues with pulsed power

sources restricted the expansion of this early technology for nearly 70 years. According to Snow and Kolm, Professor Edwin F. Northrup proposed the first recorded EML application for transportation purposes into space in 1937. His concept claimed to transport two people around the Moon using EML technology. Throughout most of the 20th century, research on EML continued to focus on transportation applications, including catapults for aircraft carriers and high-speed ground transportation. Research expanded into Japan and Germany in the early 1970s (Snow & Kolm, 1992).

Snow and Kolm presented historical information confirming that the first time EML technology was applied to space research by the United States Government was from 1975 through 1977 at NASA Ames, in Mountain View, California. During this time, NASA conducted three summer studies into a mass driver design capable of launching payloads up to 10 kg in size at 10 per second (Snow & Kolm, 1992). William Jacobs and Justino Montenegro's article showed that in the 1990s, NASA pivoted towards horizontal linear-motor tracks to magnetically levitate vehicles as an alternative to chemical rockets. According to them, these systems would theoretically be capable of overcoming the required escape velocity, between 9.447 and 9.730 km/s, for the intended orbital altitude and transport payloads into orbit.

Later, in the early 2000s, the Kennedy Space Center and the Advanced Space Transportation Program (ASTP) developed a 12.2-meter magnetic levitation (MagLev) sub-scale proof-of-concept track to assist during the first stage of launch. If built to scale, the system can replace 20% of the mission's fuel budget (Jacobs & Montenegro, 2000). As described by Wright et al. in a paper published in *IEEE Transactions on Plasma Science,* the full-scale track, envisioned in Figure 2, was never built. However, smaller EML test tracks were created at NASA installations across the country to prove that the concept was feasible at a small scale. The United States is currently not funding further research into terrestrial EM launch systems (Wright et al., 2011).

Figure 2. Concept Drawing for a Hypersonic Flight System Launched from EML Track at Kennedy Space Center. Source: Starr (2010).

2. History of NASA Research in Lunar-Based Electromagnetic Launch

Applying terrestrial EM launch capability to moon-based operations was a natural progression for NASA; while Earth-based EM launch systems compete with atmospheric drag and gravitational losses, LEML systems could benefit from the Moon's lack of atmosphere and lower gravity. In 1961, a study conducted by NASA Langley Research Center in Hampton, Virginia, focused on building a linear synchronous motor coilgun capable of supporting future lunar bases. As reported by Snow and Kolm in 1992, this technology was quickly replaced by research into mass drivers, now referred to as railguns, in the 1970s. The Massachusetts Institute of Technology (MIT) Francis Bitter National Magnet Laboratory research group constructed the first proof-of-concept-launcher model in 1977. However, this type of system's benefits can be disputed due to the energy storage capacitors used in this design having a low energy density (Snow & Kolm, 1992).

As NASA continues to work towards returning to the Moon and eventually Mars, the concept of using a LEML for fuel transportation remains a viable option. NASA has studied different configurations and designs of LEML that would best suit the proposed mission of launching fuel into lunar orbit. Unlike on Earth, mechanical components would have to be launched from Earth and brought to the Moon to be used as intended. This additional cost and use of chemical rockets will need to be factored into the concept's total

cost. Like all new NASA technologies, a LEML system's development process would fast track terrestrial uses for this technology. The use of LEML technology terrestrially was explored by Wright et al. in their paper published in *IEEE Transactions on Plasma Science*. They postulate that LEML technology would provide an environmentally clean option for Earth-based transportation, as well as having space-based uses. They concluded that any application with the potential of replacing fossil-fueled transportation is worth investigating, and problems solved for lunar missions can be equally used to solve Earth's problems (Wright et al., 2011).

3. Proposed Electromagnetic Launcher Designs

Electromagnetic launch can be achieved in several different ways and, numerous EML designs have been developed over the last century. As published in *IEEE Transactions on Plasma Science by* Ian R. McNab, the two primary categories of launch techniques considered for use on the Moon include the railgun and the coilgun (2013). This research suggests that railguns are best launch method for this mission set; however, research conducted over the last several decades has come to varying conclusions. Understanding what launch conditions are required to send payloads of raw, lunar, chemical compounds from the moon's surface into orbit will add to the body of research surrounding which EML system is the most fitting for this problem. Both the railgun and the coilgun designs have been briefly described below.

a. Railgun Principles

A railgun is a mechanism that uses electromagnetic forces to accelerate an armature between two conducting rails. This device has three components: the pulsed power system, a barrel, and an armature. The barrel is comprised of two conducting rails that generate a magnetic field. A Lorentz force is caused when the current runs down one rail, crosses through the armature, and back through the adjacent rail (McNab & McGlasson, 2020). This force then pushes the armature through the barrel, and we defined the Lorentz force by:

$$\vec{F} = \vec{I}l \bullet \vec{B}\,, \tag{2}$$

where:

F=Force
I=Current
l= armature conduction path
B= Magnetic field.

A pulsed power source supplies current for the rails, which produces the magnetic field around the rails. Force is a product of the current multiplied by the length of the armature conduction path and crossed with the magnetic field. The magnetic field is optimized by using conducting material and propels the armature in a forward motion down the barrel. We can use the right-hand rule to visualize the resultant force from the cross product of current and magnetic field, as displayed in Figure 3.

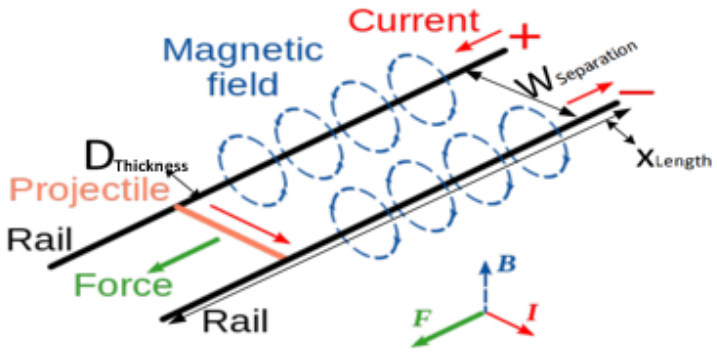

Figure 3. Rail Gun Model. Source: Stewart (2016).

The launch force can also be expressed as the square of the current and the inductance gradient of the rails, as seen in the "railgun" equation

$$F = \frac{1}{2} L' I^2 \quad , \tag{3}$$

where:

F=Force on the armature
L′=inductance gradient (Henries per meter)
l= current (Amperes).

Railguns are proven to achieve higher launch velocities than coil guns and linear motors. According to Ian R. McNab in a paper published in *IEEE Transactions on Plasma Science* in 2013, railguns have demonstrated the ability to exceed 2000 m/s when launching payloads of 10 kg and velocities over 4300 m/s with masses of 0.6 kg. The ability to meet and potentially surpass the required lunar escape velocity with additional stages makes this method enticing for further research.

b. Coilgun Principles

In their 1992 article, Snow and Kolm define coilguns as a type of EML that generates thrust between two or more coils in close proximity to each other. Coilguns consist of a current-carrying projective coil that passes through a current-carrying barrel coil. These components can be configured coaxially or coplanar to each other but must be inductively coupled together. The coil currents' product multiplied by the proportionality constant, or mutual inductance gradient between the projectile and barrel coils, generates thrust (Snow & Kolm, 1992). In a contractor report from 1990, Nathan Nottke and Curt Bilby expand upon the coilgun's science. They reported that synchronizing the current in the barrel coil with the projectile as it passes provides the acceleration force. According to them, the system minimizes the energy lost from conductor heating by utilizing a pulsed power source to provide current. The storage time interval equals the coil's inductance divided by the material's resistance (Nottke & Bilby, 1990).

The coilgun design discussed by Snow and Kolm can achieve on the order of megajoules of launch energy required of LEML system but require inductive energy storage, replacing traditional larger capacitors that do not have the required energy density. Inductively stored energy is challenging to commutate or turn the coil current on and off. According to Snow and Kolm, additional techniques, such as projectile brushes, could maintain the barrel current but could cause problems with large energies in a lunar environment (1992). One coil gun design, as described by Nottke and Bilby, is shown in Figure 4.

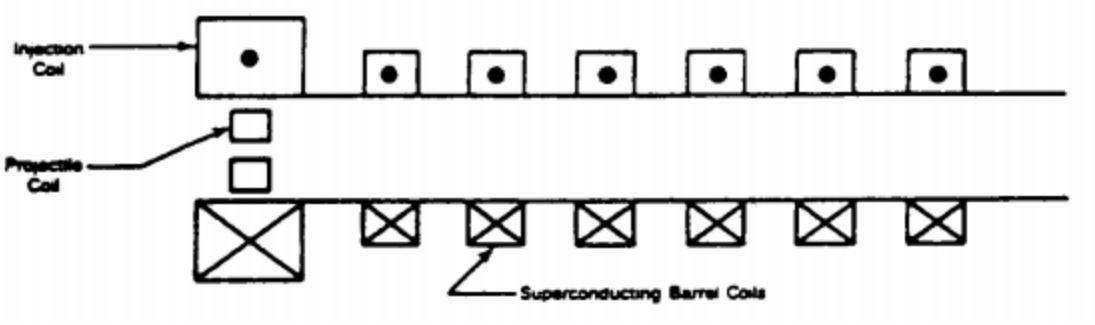

Figure 4. Design for a Coilgun Varient Known as Quenchgun
Source: Nottke and Bilby (1990).

As Snow and Kolm reported, coilguns have only reached 1000 m/s in a demonstration (1992). A payload would not reach the lunar escape velocity of 2.38 km/s unassisted with a launch velocity of 1 km/s. Instead, the payload would require a kick motor, reducing the payload's storage capacity. Ian McNab's research observed that the payload's required geometric shape would hinder the use of a coil gun launcher. According to him, the coil gun bore design will prevent the LEML from launching larger sizes and masses required of the lunar- payload (2013).

c. Comparing Coilgun to Railgun

It is important to note that much of the research conducted on these alternative launching techniques remain theoretical. The concepts that drive the coilgun and synchronous motor designs have been built on a micro-scale; however, neither has exceeded one km/s in launch velocity. In comparison, significant progress has been made in improving railgun technology. The Navy has explicitly built functional railguns that achieve the velocities required by a LEML discussed in this research.

C. ARTEMIS

In 2017, when it announced the NASA Artemis program, the United States established a new era of human lunar exploration. As revealed in NASA's Lunar Exploration Program Overview, published by the administration in 2020, this mission brings together the country's thriving space industry, academic centers of excellence, and international partners, and provides a unifying mission of returning to the Moon by 2024.

Additionally, the program intends to develop and test the infrastructure and processes for human travel to Mars. According to the overview, the Artemis mission will use NASA's Space Launch System (SLS) rocket and the Orion spacecraft to return humans to the Moon after a series of uncrewed and crewed test flights into low-Earth, high-Earth, and lunar orbits. The project also includes a long duration, permanent presence, both in lunar orbit and on the Moon's surface. The orbital space station, known as the Gateway, is a large part of the initial lunar architecture. This outpost is considered a critical component of NASA's means of achieving sustainability while operating in the lunar environment (NASA, 2020a).

1. Artemis Accords

In May of 2020, delegations from Australia, Canada, Italy, Japan, Luxembourg, the United Arab Emirates, the United Kingdom, and the United States of America signed the Artemis Accords, a document intended to solidify international cooperation regarding the peaceful use of the Moon through the Artemis program. This multilateral agreement described the responsibilities of international partners. Its intended purpose was to bolster the 1967 Outer Space Treaty (Potter & Warner, 2020). Space Resources was among the ten principles outlined by the Artemis Accords. Section 10 discusses the benefits of extracting and utilizing resources in long-duration space habitation. They emphasized the requirement to ensure sustainable practices while adhering to the Outer Space Treaty (NASA, 2020b). The Artemis Accords authorizes the utilization of lunar resources to continue human space exploration and allows the United States to continue to explore means of extracting and exporting lunar ice off the surface of the Moon and into lunar orbit for use as fuel for future missions.

2. Lunar Gateway

As described by the Lunar Exploration Program Overview (2020a), the Gateway space station will serve as a launch point for astronauts before they descend to the lunar surface. The space station will serve as a refueling point for the lunar lander and be used to simulate long-duration missions, such as the eight-month trip to Mars, from a relatively safe distance from Earth. In the long term, the first crews traveling to Mars will use the

Gateway as a critical resupply point for more extended space exploration missions. The Gateway also may be used as a possible intercept point for refueling and a destination for our LEML payload (NASA, 2020a). Its primary purpose is to support crew members and augment life support provided by the Orion space capsule. The station also provides "command, control, and data handling capabilities; energy storage and power distribution; thermal control; communications and tracking capabilities" (p. 24). As seen in Figure 5, the Gateway will initially consist of a Power and Propulsion Element (PPE), made by Maxar Technologies, and the Habitation and Logistics Outpost (HALO), developed by Northrop Grumman. The two sections will be assembled on Earth and launched on a single rocket (p. 10). Docking ports are included in the design to be compatible with the Orion capsule and SpaceX's Dragon Capsule, currently contracted to conduct resupply missions. The international community has submitted proposals for several scientific payloads on the space station. These experiments will be autonomous and have established interoperability standards, agreed upon by international partners, to allow for further collaboration within the scientific community (p. 24). As the Artemis mission unfolds, the Gateway will play a critical role in the planned surface exploration demonstrations.

Figure 5. Lunar Gateway Concept Art. Source: NASA (2020a).

a. Selecting an Orbit for the Gateway

Like Earth, the Moon has several orbital regimes in which a space station can reside. NASA considered several of these orbits, including Butterfly Orbits, Distant Retrograde Orbits (DROs), Halo Orbits, seen in Figure 6, and Low Lunar Orbits (LLOs), before selecting the best one that meets the objectives of the Artemis program. These orbital families each provide unique benefits and drawbacks regarding a long-duration crewed mission. The Gateway would require accessibility from Low Earth Orbit (LEO), minimum time spent in Earth and the Moons penumbra, and be accessible to the southern lunar pole for mission support of the surface. After extensive consideration, a Near-Rectilinear Halo Orbit (NRHO) met each of the mission requirements outlined, and NASA selected it as the Gateway program's operational orbit in 2019.

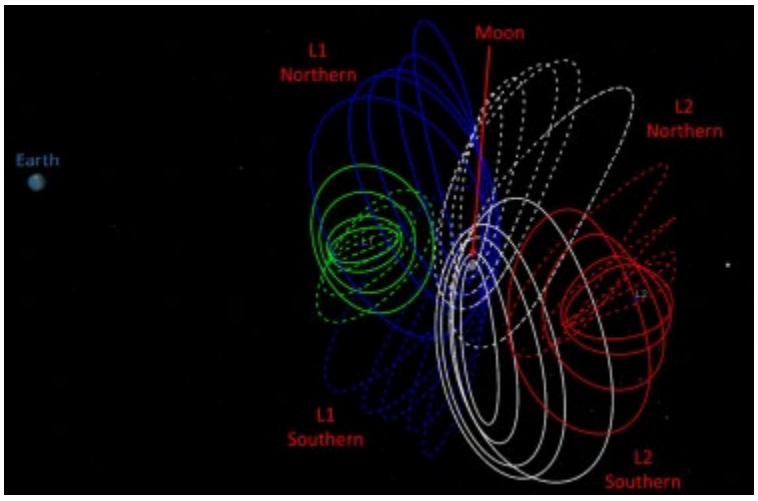

Figure 6. Halo Orbit Families in the Earth-Moon System.
Source: Lee (2019).

b. Benefits of Near-Rectilinear Halo Orbit

The Near-Rectilinear class of orbits exists in any three-body system with two gravitational entities. According to Zimovan et al. in a paper presented at the 3rd IAA Conference on Dynamics and Controls of Space Systems, both the Earth and the Moon's strong gravitational attraction influences the orbit's shape (2017). Their research noted that these orbits are also approximately bounded by the liberation points L_1 and L_2, which make

their fundamental behavior relatively stable. These orbits also extend in both the northern and southern planes. Advantages of the NRHO include low-cost transfer orbits to Earth, the lunar surface, and deep-space. Zimovan et al. indicated that this orbital regime also provides beneficial properties for avoiding eclipses caused by the Earth and Moon (2017).

In a 2019 NASA white paper, David E. Lee suggested that scientists considered L_1 and L_2 Lagrange points and their associated mirrored northern and southern orbital families for the Gateway's orbit. According to Lee, the southern L_2 NRHO proved most favorable for several reasons. NASA selected the southern family of orbits because the Orion capsule will be traversing from Earth's northern hemisphere to reduce the required ΔV for the journey. This orbital regime also provides the best communication coverage with the southern pole, the lunar base's proposed location. Lee adds that there are many orbital shapes within the halo family; NRHOs have stable characteristics with the potential to decrease the amount of necessary maintenance propellent, ΔV, and overall operational costs (Lee, 2019).

Another determining factor in selecting this halo orbit is its ability to avoid eclipses. According to Zimovan et al., the orbit's geometric pattern is perpendicular to the orbital plane, and objects in this orbit avoid passing through the Earth's penumbra or shadow. Zimovan et al. ascertain that avoiding Earth's penumbra is favorable both in terms of power and communication. By avoiding the Moon's far side entirely, the Gateway can maintain contact with Earth longer without interruption. Communication between the station and the lunar settlements at the south pole will also have extended contact periods in this orbit (Zimovan et al., 2017). Achieving continuous communication with settlers on the southern pole would require combining coverage with a communication satellite in the complementary phasing slot, a consideration NASA should have when designing the final mission.

THIS PAGE INTENTIONALLY LEFT BLANK

III. METHODOLOGY AND MODEL DESIGN

In terms of space exploration, models and simulations are vital in enhancing decision-making; when used effectively, engineers can visualize launch conditions without first bringing equipment to the Moon for testing. Designing and building a LEML capable of successfully cycling raw materials from the moon into orbit requires understanding the necessary power, energy storage requirements, and length of the barrel needed to accomplish this mission. These physical constraints can be calculated after modeling the ΔV required to launch a payload from the Moon's surface and intercept with the Gateway. Without flight hardware on orbit around the Moon to test our thesis statement, it was necessary to create a realistic, high fidelity model to determine the required launch parameters for a LEML payload intercepting the Gateway's orbital path.

A. DESIGN

Determining the modeling software to use was the first step in creating a model capable of producing results to confirm our thesis statement. Modeling software considered for this problem included Microsoft Excel, MATLAB, and STK. The requirements outlined in this thesis and the ability to leverage the astrogator feature on STK resulted in this software being selected to create and analyze this model. Developed by Analytical Graphics, Inc. (AGI), STK is a physics-based platform used to visualize and analyze missions involving spacecraft, aircraft, ships, and sensors in modeled 2D and 3D environments. This thesis's STK simulation used the Naval Postgraduate School's license for unfunded educational research and STK version 12.

1. Components

Defining this model's essential requirements became the next step in development. The STK model was designed with three primary components: the payload launched from an electromagnetic launcher, the Gateway reference trajectory, and the planetary bodies affecting the modeled system.

a. Lunar Electromagnetic Launcher

In the model, the proposed LEML was placed at the lunar south pole to match the lunar base's suggested site as described by Artemis's proposal (NASA, 2020a). For simplicity, the LEML was placed at the exact cartesian southern pole. The model was able to simulate launching a payload at varying velocities, angles, and elevations to determine the position and speed at which the LEML would intercept the Gateway's path at various points on the NRHO. The initial four locations on the orbit that were targeted were the 0°, 24°, 90°, and 270° azimuths, in which azimuth is referenced to lunar X, towards the positive Y plane. These points included: mid-points near the Moon's equatorial plane (0° and 24°), the nearest point (90°), and the farthest point (270°).

To model the launch conditions of the LEML, STK's Astrogator propagator was used. Astrogator is a high-fidelity numerical integration propagator used for trajectory and maneuver planning and is the best propagator for realistic problem sets. The targeting feature allowed the LEML payload to target the Gateway and narrow down the independent variables of azimuth, elevation, magnitude, orbit epoch, and trip duration of the LEML. These variables were analyzed to determine what parameters were required to allow the LEML to intercept the Gateway's orbit at various points along its trajectory. The targeting sequence was nested with an initial state, a maneuver segment, and a propagate segment.

(1) Initial State

The STK software was not designed to replicate an EML on the moon's surface. Instead of modeling the launcher's exact parameters as a launch segment in STK's Astrogator, the location of the LEML was inputted as an initial state inside of a targeting sequence. The targeting sequence used a differential corrector to target the Gateway's position and time. The initial state placed the LEML at the lunar south pole at an altitude that matched the moon's polar radius, 1736.0 km (Williams, 2020).

As the LEML was modeled as an initial state, initial conditions were coded into the astrogator as best guesses for the resulting launch parameters. The LEML launch location on the Moon's surface was put into the initial state using Cartesian coordinates. The launcher was placed at the lunar south pole's exact center on the surface, as seen in Figure

7, which provided freedom of maneuver in all 360 degrees to find the optimal launch conditions.

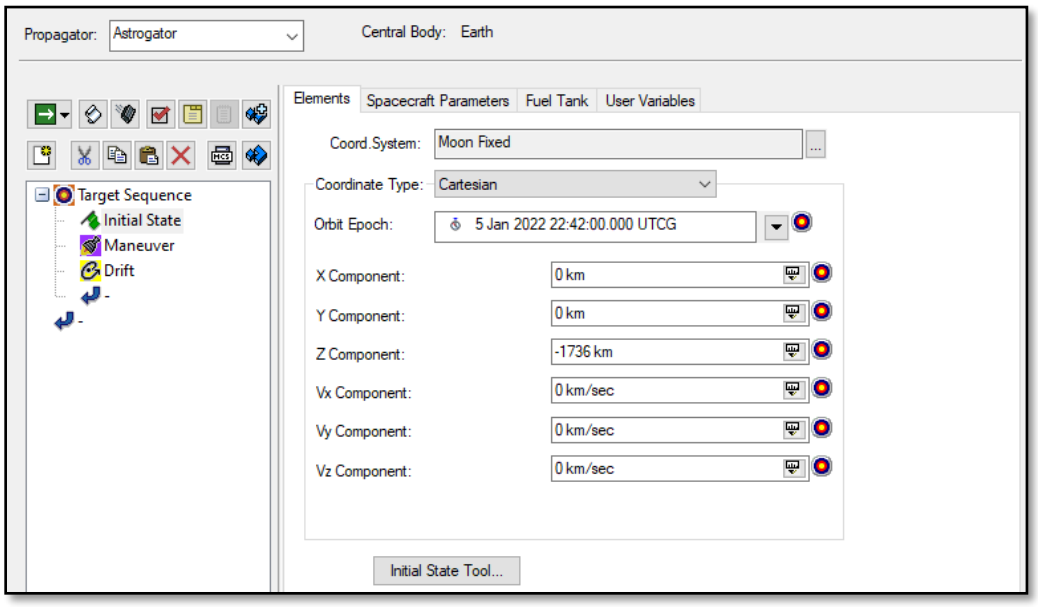

Figure 7. The Initial State of the Target Sequence

The payload's parameters were also defined in the initial state, and were set to have a dry mass of 70 kg as a reasonable prediction based on the payload design, including packaging and the ice (I. McNab, email to author, January 8, 2021). This was just an initial estimate used throughout the investigation. The model could easily be adjusted to replicate results at various masses. All other spacecraft parameters were left as default values, as seen in Figure 8.

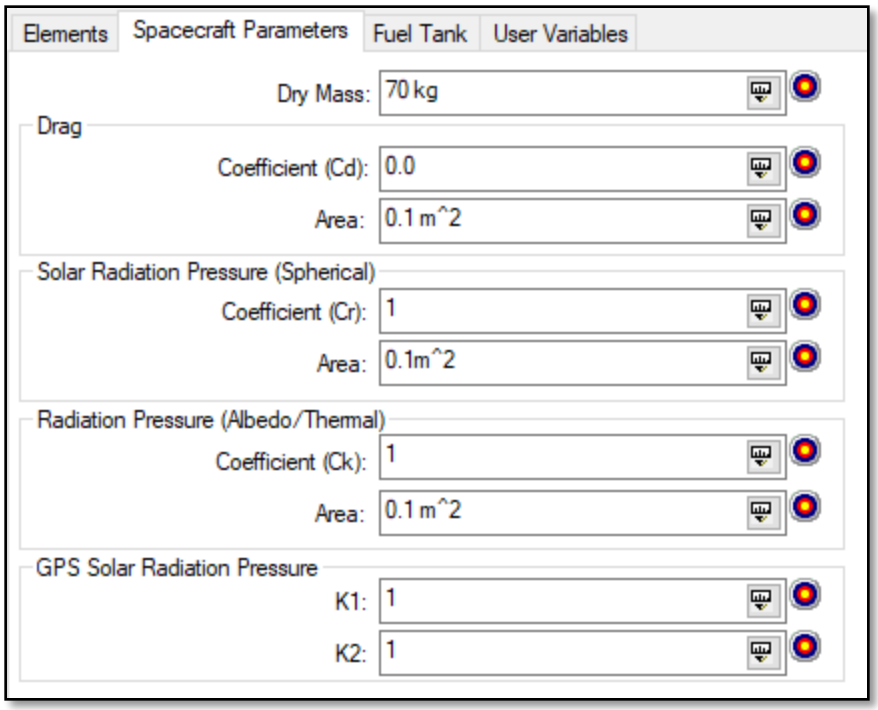

Figure 8. Spacecraft Parameters for the Payload

In order to calibrate the model to target points along the trajectory, a best guess for time of flight was required to postulate the launch epoch and duration. Initially, the problem was treated as a traditional co-planer transfer, in which a spacecraft completes a burn out of a parking orbit and into a higher orbit, as depicted in Figure 9. In this case, the initial state was used as the parking orbit. The time of flight (TOF) calculation, seen in (4), was used to determine the estimated epoch time for the LEML to be launched from the lunar surface:

$$TOF = \frac{P}{2} = \pi\sqrt{\frac{a^3{}_{transfer}}{\mu}} \quad . \tag{4}$$

Though not circular, the NRHO was treated as a circular orbit at the reference points closest to the orbit's apolune. The time of flight for the LEML's trajectory was calculated using the spacecraft's location, as provided by the azimuth, elevation, and range report (AER). These calculations provided an initial guess regarding the trip duration. Knowing at what

time the Gateway would be passing through the target point on the NRHO also meant that the launch epoch could also be estimated.

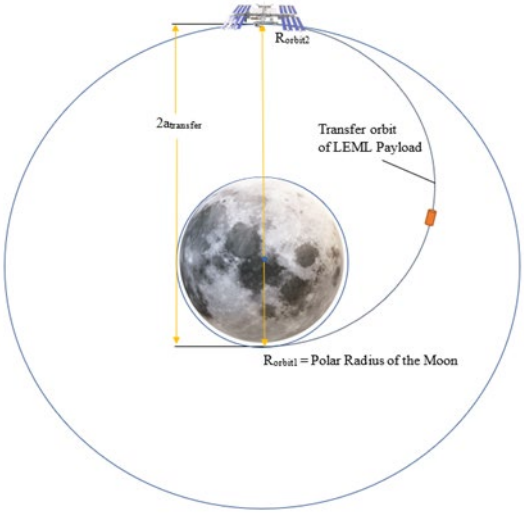

Figure 9. Example Transfer Orbit Targeting the Gateway.
Adapted from Sellers et al. (2000).

(2) Maneuver Segment

A maneuver segment was then added to the astrogator to simulate a LEML launch. Attitude control was set to thrust vector, and the thrust axis was set to the Gateway RIC coordinate system between the primary and relative objects. This axis allowed the LEML to target the Gateway's position and time during the maneuver. In the maneuver segment of the target sequence, initial estimates for the LEML's thrust vector were selected. Because the study aimed to estimate the azimuth, elevation, and magnitude required to intercept with the Gateway, the spherical coordinate system was used; however, it also auto converts to X, Y, Z thrust vectors. A modest estimate of 2300 m/s was used as an initial parameter, as seen in Figure 10. The initial estimate was driven by the escape velocity of the Moon, calculated in chapter 2 to be 2380 m/s. The payload would remain in orbit around the Moon to intercept with its target. Other conditions for the payload were also set in the maneuver segment. The engine was modeled to have a constant acceleration and specific impulse, I_{SP} to replicate the launch conditions. The maneuver was also set to impulsive.

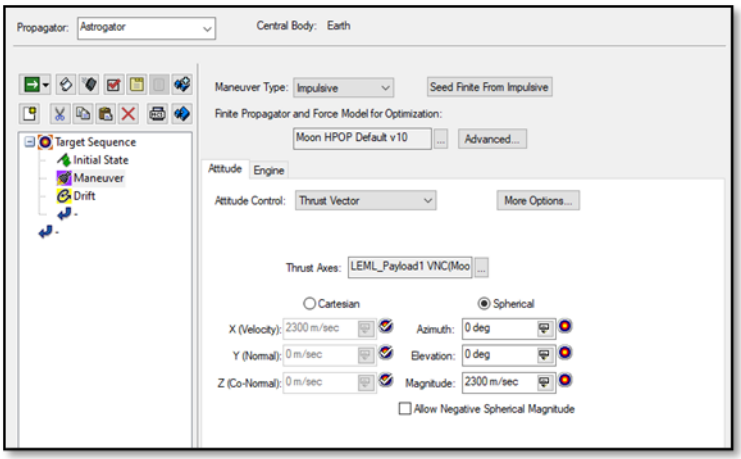

Figure 10. Maneuver Segment of the Target Sequence

The finite propagator and force model used in the maneuver segment of the LEML payload was the Moon High-Precision Orbit Propagator (HPOP) Default v10. According to STK, this propagator is also a high-fidelity orbit propagator that "generates ephemeris using numerical integration of the differential equations of motion" (STK, 2021a, para. 1). Specifically, the Runge-Kutta-Fehlberg method of order 7–8 numerical integration was used in this model.

(3) Propagate Segment

A propagate segment was the final segment added to the targeting sequence, which allowed the payload to continue its trajectory after the initial maneuver. In this scenario, the propagate segment was labeled the drift to indicate that the spacecraft will drift after its initial launch. A stopping condition was used to stop the sequence once the payload reached its apoapsis, giving the spacecraft enough time to propagate between launch and interception with the Gateway. The drift segment also used the Moon HPOH Default v 10 propagator.

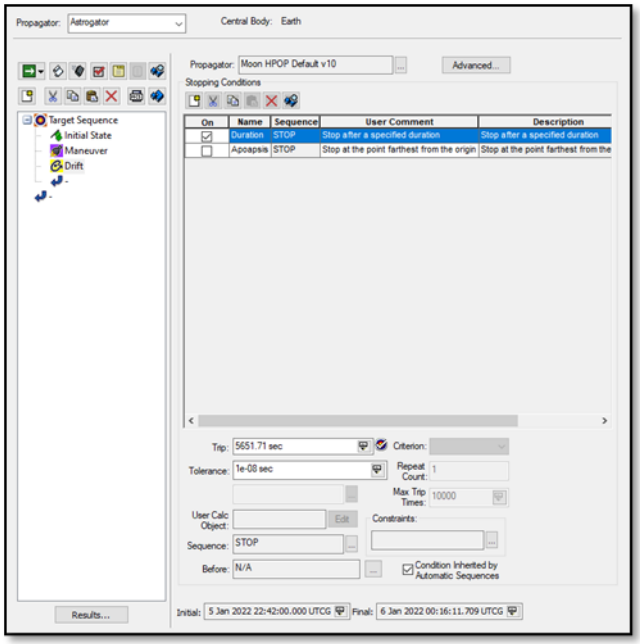

Figure 11. Propagate Segment of the Target Sequence

b. Lunar Gateway Reference Trajectory

The specific NRHO selected by NASA for the Gateway was the L2 southern family with a period of 9:2 Lunar Synodic Resonance (LSR), meaning the orbit will average nine revolutions every two lunar months. The average orbital period is 6.562 days (Lee, 2019). The obit has a perilune radius of approximately 3,366 km and an apolune radius of roughly 70,000 km. Although relatively stable, spacecraft in this orbit will experience perturbations from solar pressure and gravity gradient at perilune. The Gateway will require orbit maintenance maneuvers (OMM) during long-duration operations to prevent the space station from departing the lunar vicinity (Newman et al., 2018).

NASA's Gateway NRHO reference trajectory, seen in Figures 7 and 8, was imported into our STK model from a SPICE SPK-type kernel. The space administration's information system, known as SPICE, is used by engineers to model, plan, and execute planetary exploration missions. NASA's Planetary Science Division maintains a database of data sets, called kernels, that provide navigation and ephemeris data for NASA's current and proposed spacecraft (Semenov, 2020). The sample deep space gateway orbit file contained the spacecraft, Earth, and Lunar ephemerides as a given function of time. The

reference file was a 15-year near-continuous orbit with a start date of 2020 JAN 02 08:09:36 through 2035 FEB 11 03:59:59. The kernel referenced was found at the Jet Propulsion Laboratory's Planetary Data System Navigation Node JPL website (Whitley et al., 2018).

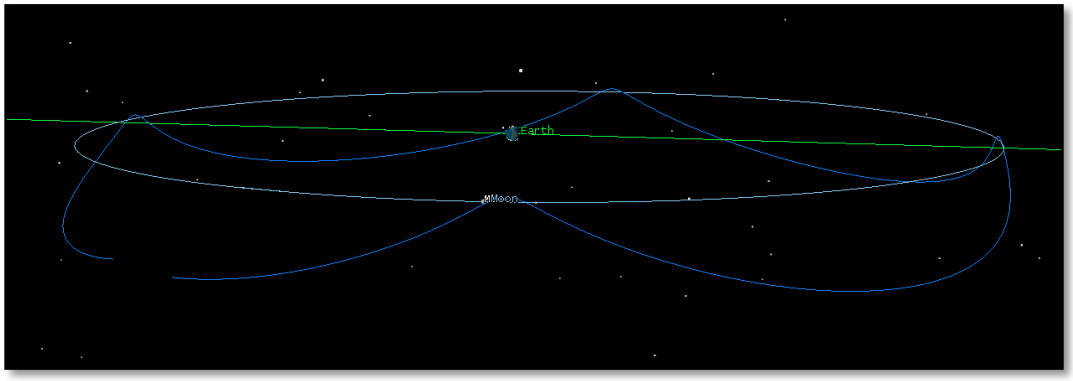

Figure 12. STK Model of NRHO Earth-Centered Reference Trajectory

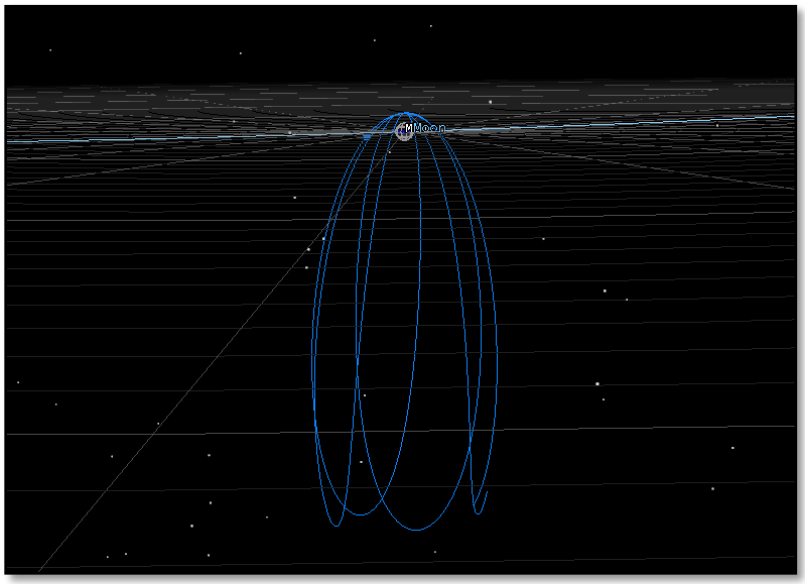

Figure 13. STK Model of NRHO Moon-Centered Reference Trajectory

c. Planetary Bodies

Our modeled environment consisted of the three bodies: Sun, Earth, and Moon system. Although other gravitational bodies in the solar system, such as Jupiter, would be expected to affect this system, they were not included in this study. Both the LEML trajectory and the NRHO SPICE file have Earth as their central body.

2. Reference Frame

The reference frame used in this model was Earth J2000. The frame is defined by the Mean Equator and Mean Equinox as defined by referenced astrometric data from the 50-year epoch, specifically 1 January 2000 12:00:00.000 TDB (STK, 2021b). It was essential to ensure that the NRHO orbit and the payload's trajectory were in the same reference frame. The kernel provided was in an Earth-centered reference with the J2000 coordinate system. The payload trajectory needed to match to ensure the Gateway and payload's rendezvous occurred in the same reference frame.

3. Perturbations

This model intended to create an idealized reference trajectory to support initial calculations involving required launch conditions. Specifically, the NRHO reference track was created to be a generic representation of the course of the spacecraft over time. The only perturbations considered in its design were the n-body gravitational model inherent to the ephemeris data (Lee, 2019). Other perturbations could be considered in future research: solar pressure, drag, and spacecraft noise inherent to space vehicles. Other considerations such as navigational errors, insertion errors, and orbit maintenance maneuvers will also need to be considered in future models but were not considered in this research (Lee, 2019). The force effects applied in the Moon HPOP propagator include gravitational losses from the central body and the Moon, the spherical solar radiation pressure model, and Third Body forces from Sun and Earth.

B. DATA ANALYSIS

To answer the proposed problem statement, STK was used to visualize the launch parameters required to intercept the NRHO at various points. Reports generated by the

scenario were used to analyze where the orbiter and the payload were located for the launch sequence duration. An AER report was used to locate the Gateway along its trajectory. The MCS summary and RIC reports were used to analyze the rendezvous' success. The residual velocity and direction of the payload at rendezvous will also be compared to the Gateway's relative position and velocity. The delta between these figures determines the need for additional thrusters to perform docking procedures.

C. ASSUMPTIONS

The Artemis program is a proposed mission and is still in the planning phase of its conception. Because this analysis is working off the current parameters of the mission architecture from NASA's plans, it is expected that many of the assumptions made in this research may change over time. Deductions have been made and applied to this model based on the architecture as it is currently presented. Parameters, such as orbital regime, speed, and size of the Gateway, and the size, mass, and contents of the payload used in this scenario are subject to change, knowing that these assumptions may be further refined by NASA in the future.

IV. RESULTS

The model created for this research allowed manipulation of the five independent variables: launch epoch, spherical thrust coordinates (azimuth, elevation, and magnitude), and trip duration, to target and intercept the Gateway's radial, in-track, and cross-track relative position along the NRHO at multiple points. Next, the model leveraged the astrogator propagator and the use of a differential corrector at each designated point, to narrow down the optimal launch parameters and determine the lowest possible final velocity upon intercept. The program then generated reports depicting the two object's relative positions and fixed velocities at rendezvous. Lastly, these reports were analyzed and used to narrow the differential correctors' best guess calculations, to determine the point along the orbital path with the lowest relative intercept velocity. Other scenarios observed included incremental launches based on time and the LEML's ability to launch with fixed azimuth, elevation, or magnitude.

A. LOCATING THE GATEWAY

STK's AER data described the Gateway's location along the NRHO in relation to the Moon as a fixed body. This data presented the space station's azimuth, elevation, and range to determine the spacecraft's relative position to the center of the Moon's default local X, Y, Z axes. The initial four locations on the orbit that were targeted were the 0°, 24°, 90°, and 270° azimuths, in which azimuth is referenced to lunar X, towards the positive Y plane. These azimuths represent the points in which the Gateway approaches the lunar equator, passes the lunar equator, passes directly above the lunar north pole at the apolune, as well as at the spacecraft's perilune. The AER report results for the four targeted locations are presented at a scenario time with an interval of 60 seconds, as displayed in Table 1. This data provided the time in which the spacecraft passed these four specified points. With estimates for the trip duration and the epoch calculated, a target sequence within STK's astrogator was populated. The first of the four orbital positions to be targeted was the third on our list, the 90° azimuth. The orbit epoch was calculated to be 5 Jan 2022 22:42:00.000.

Table 1. Moon AER Data and calculated Payload Time of Flight

Intercept (UTCG)	Azimuth (deg)	Elevation (deg)	Range (km)	TOF (s)	Epoch (UTCG)
1/5/22 20:45	359.935	-4.979	11043.666	22917.227	1/5/2022 14:09
1/5/22 22:25	24.332	-2.472	6360.076	11555.658	1/5/2022 19:05
1/5/22 23:49	89.542	1.924	3289.510	5651.709	1/5/2022 22:42
1/9/22 7:14	268.808	-21.233	71545.177	314681.703	1/8/2022 16:12

With the initial launch parameters set within the astrogator, the mission control segment was then run as a nominal sequence. This action was run several times running only the parameters as depicted in the target sequence. The spherical thrust vector was adjusted incrementally until the payload came into range of the Gateway. The azimuth was adjusted in increments of 10° while the magnitude was adjusted in increments of 100 m/s. Once the payload approached within 1000 km of the Gateway, incremental changes within 1° and one m/s were made to better target the payload. The Gateway and payload's AER and fixed position were monitored during the iteration, and visual observation was also conducted to determine if the targets were getting closer together or farther apart. The best result for the 90° azimuth target was approximately 200 km separation as seen in Figure 14. This result was achieved using the thrust vectors represented in Figure 15.

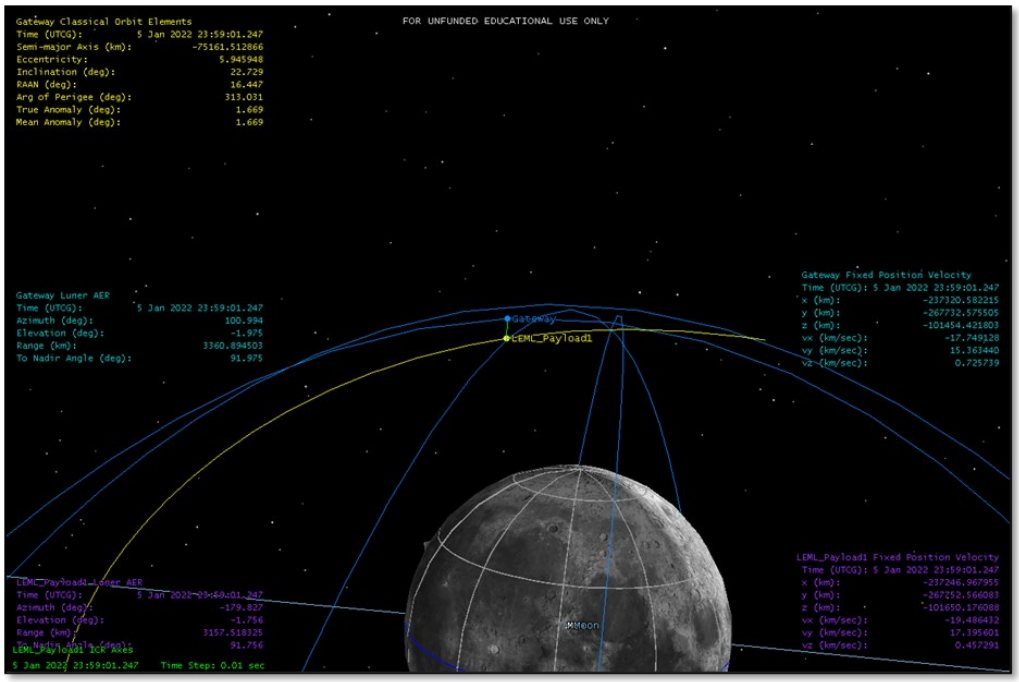

Figure 14. 3D Visualization of Close Approach Between Gateway and Payload Near 90° Azimuth

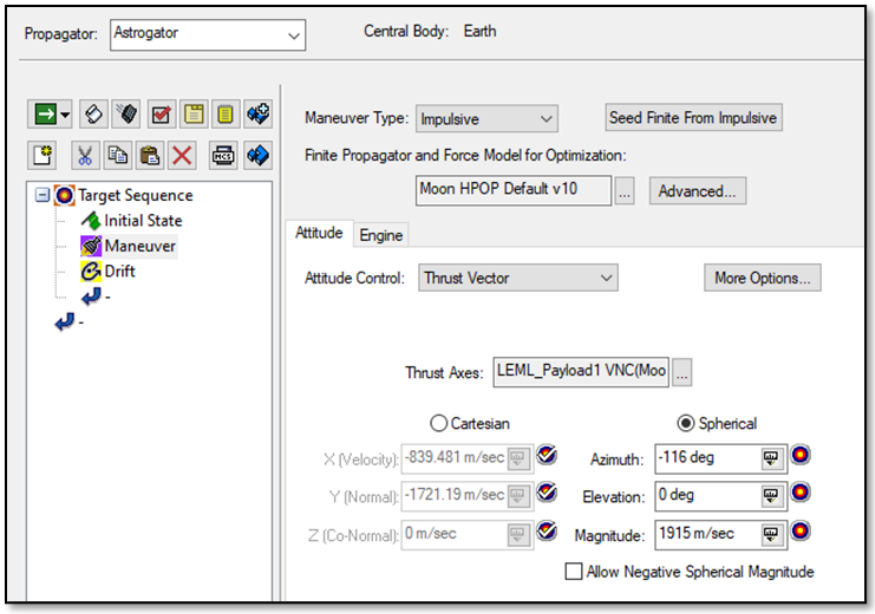

Figure 15. Maneuver Segment Thrust Vector Used to Target Position 3

B. DIFFERENTIAL CORRECTOR

With an initial estimate for the thrust vector, the differential corrector was ready to be utilized. Within the drift segment, the dependent variables were selected. These included: radial, in-track, and cross-track. Each variable was configured so that the Moon was selected as its central body. Their reference satellite was also set to be the Gateway, as seen in Figure 16.

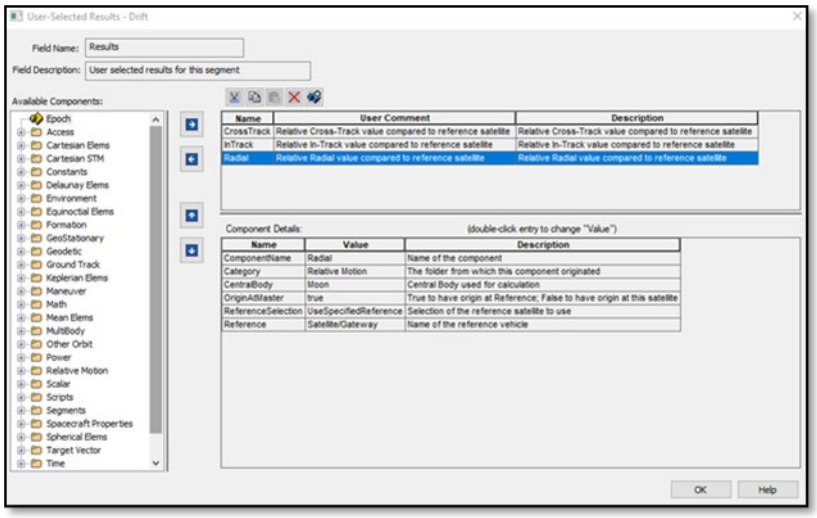

Figure 16. Selected Results for Propagate Segment

A differential corrector was then created within the target sequence. The control parameters were set to be the X, Y, and Z thrust vectors, with a max step of 100 m/s and a perturbation of 10 m/s. The constraints were configured to target the Gateway RIC at 0 km in all three axes. The tolerance was set to 0.0001 km to ensure that the payload truly intercepted with the Gateway. These settings are displayed in Figure 17. The corrector's convergence was set to 100 iterations to ensure the computer could run through enough trajectories, varying all three independent variables.

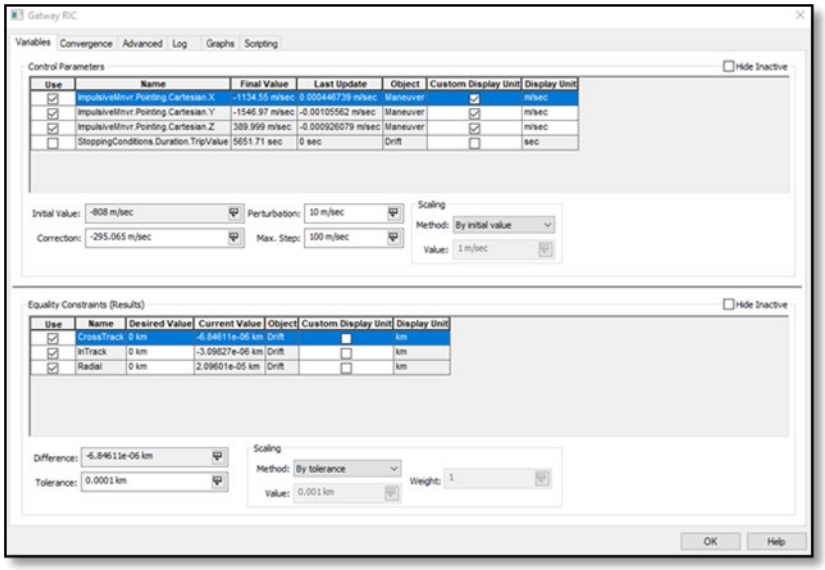

Figure 17. Differential Corrector for Target Sequence

The MCS was run with all active profiles to include the differential corrector just created. The computer then iterated trajectories until the payload intercepted the Gateway. The model completed 43 iterations before the target sequence converged, calculating new values for X, Y, and Z, as displayed in Figure 18. Figure 19 shows the 3D graphics window during the convergence, displaying the 43 attempts at convergence before the computer reached the Gateways RIC value of 0 km in each of the three axes.

Target Sequence.Gatway RIC: Finished: *CONVERGED* in 43 iterations. *Constraints Met*

Control	New Value	Last Update	Constraint	Desired	Achieved	Difference	Tolerance
...veMnvr.Pointing.Cartesian.X	-1134.55 m/sec	0.00044674	Drift : CrossTrack	0 km	-6.84611	-6.8461e-0	0.0001 km
...eMnvr.Pointing.Cartesian.Y	-1546.97 m/sec	-0.0010556 m	Drift : InTrack	0 km	-3.09827	-3.0983e-0	0.0001 km
...veMnvr.Pointing.Cartesian.Z	389.999 m/sec	-0.00092608	Drift : Radial	0 km	2.096e-05	2.096e-05 k	0.0001 km

Figure 18. EML Thrust Vector Calculated by the Target Sequence

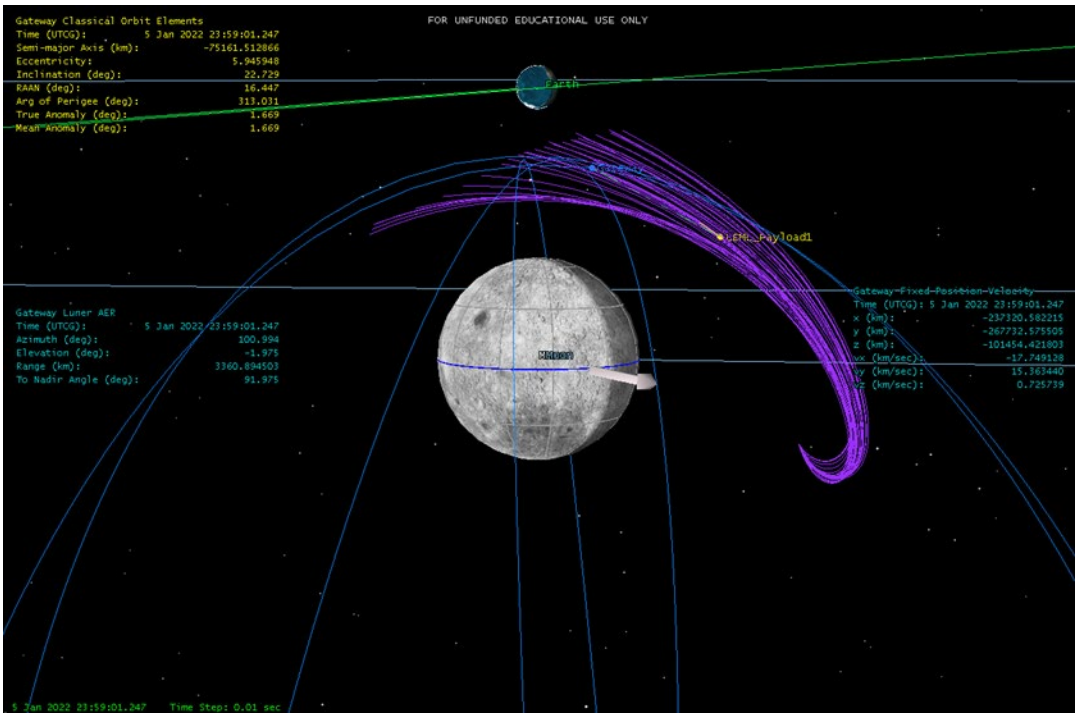

Figure 19. 3D Rendering of the 43 iterations Calculated by the Target Sequence.

Once these steps were completed, data was collected for the four original targets. The initially calculated first guesses for trip duration and epoch were used in combination with the differential corrector to target the Gateway's RIC at each location. The results of this modeling and the Gateway's RIC values at the point of intercept are displayed in Table 2. The magnitude of the Gateway and payloads terminal velocity was calculated from the fixed velocity in the X, Y, and Z directions. The difference in magnitude between the Gateway and the payload are depicted in Table 3. Figures 20–23 show the 3D graphics windows from the four target scenarios at the point of rendezvous, along with the Spacecraft's RIC data.

Table 2. Thrust Vector Results and Gateway RIC at Rendezvous

	Epoch	Azimuth (deg)	Elevation (deg)	Magnitude (m/s)	Time of Intercept	TOF (sec)	Radial (km/s)	In-Track (km/s)	Cross-Track (km/s)
1	5 Jan 2022 14:09:00.000	48.4002	57.3004	2201.15	5 Jan 2022 20:30:57.000	22917.0	0.04797	-0.62704	-0.32731
2	5 Jan 2022 19:05:00.000	48.0644	41.9992	2091.15	5 Jan 2022 22:17:35.700	11555.7	0.02037	-0.79056	-0.15164
3	5 Jan 2022 22:42:00.000	-126.256	11.4911	1957.65	6 Jan 2022 00:16:11.700	5651.7	-0.139207	-2.31877	0.657358
4	8 Jan 2022 16:10:08.069	-101.616	84.3752	2486.39	9 Jan 2022 12:35:47.336	73539.3	0.309337	0.047186	-0.76962

Table 3. Fixed Velocity at Time of Rendezvous

	Time of Intercept	Gateway Fixed Velocity (km/s)				LEML Payload Fixed Velocity (km/s)				Difference in MAG (km/s)
		Vx	Vy	Vz	V MAG	Vx	Vy	Vz	V MAG	
1	5 Jan 2022 20:30:57.000	-24.404285	-3.564439	1.639100	24.71762530	-24.594614	-3.416040	0.497298	24.8356935	0.11806821
2	5 Jan 2022 22:17:35.700	-23.463020	7.201637	-1.406962	24.58366175	-23.815199	7.506857	0.750305	24.9815845	0.39792273
3	6 Jan 2022 00:16:11.700	-16.664564	16.635087	0.342320	23.54890647	-18.306077	18.373617	0.675703	25.9453046	2.39639814
4	9 Jan 2022 12:35:47.336	29.181936	0.153589	0.428481	29.18548568	28.740653	0.340460	-0.253298	28.7437856	0.44170013

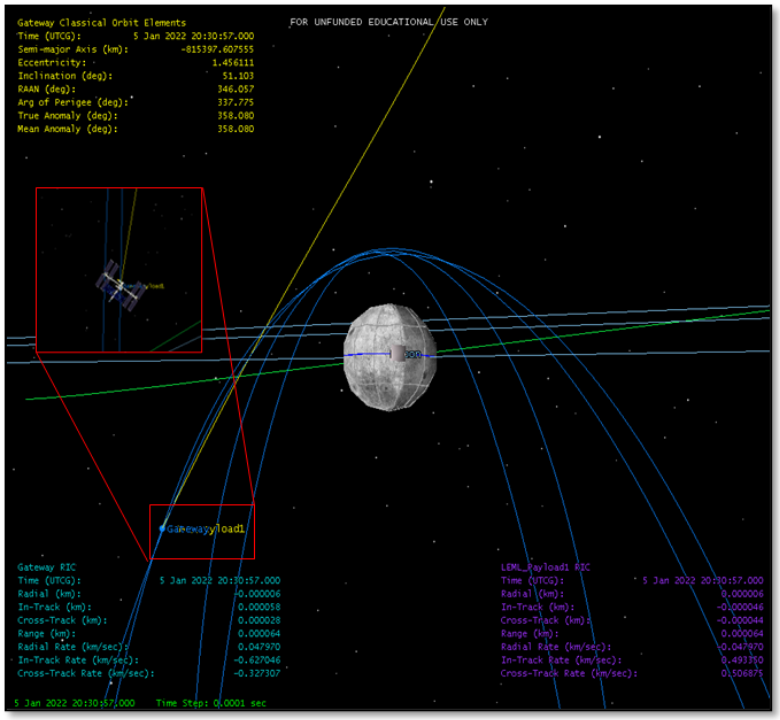

Figure 20. Target 1 at Point of Rendezvous

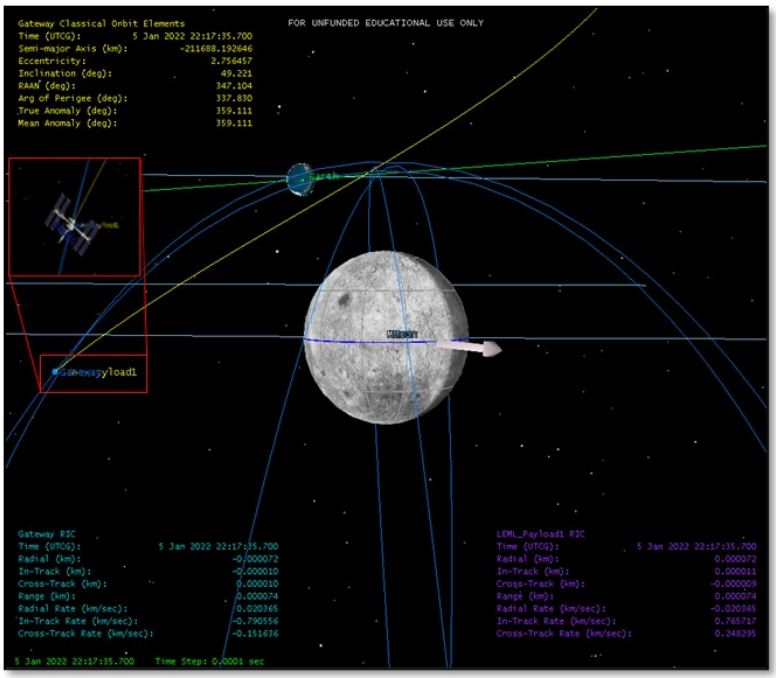

Figure 21. Target 2 at Point of Rendezvous

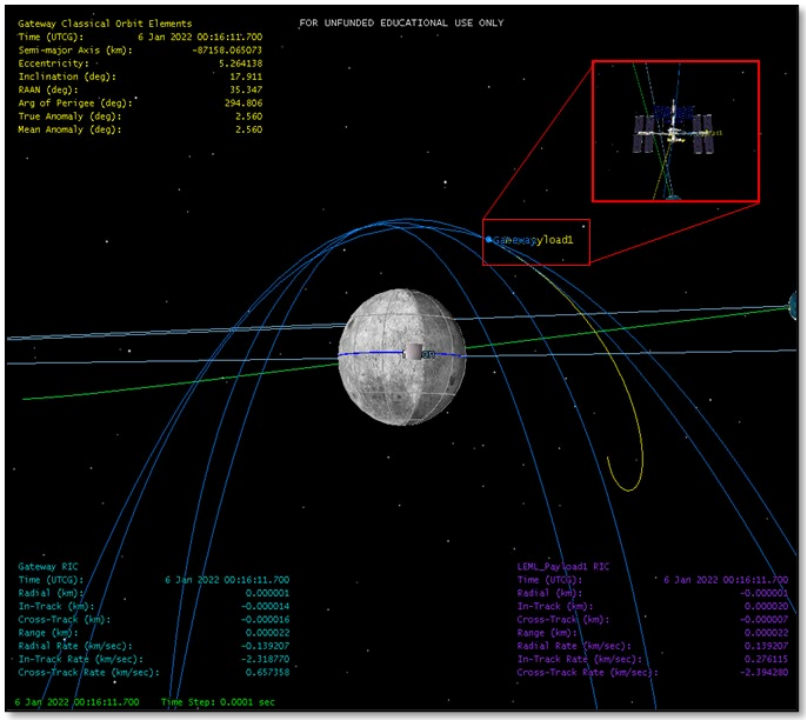

Figure 22. Target 3 at Point of Rendezvous

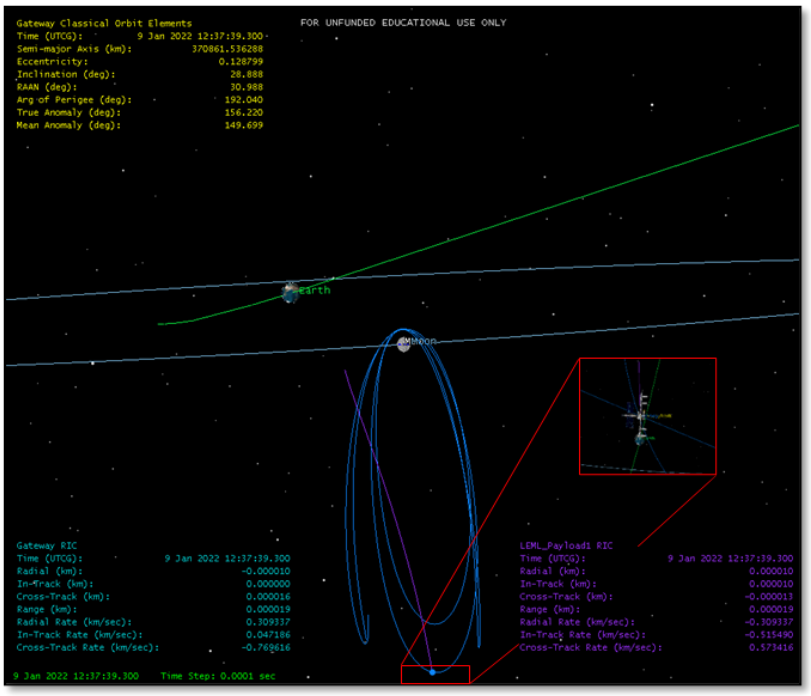

Figure 23. Target 4 at Point of Rendezvous

C. LAUNCH EPOCH

The next variable manipulated in the scenario was the launch epoch. The orbit segment between the lunar equator and the NRHO's apolune was targeted to best match the Gateway's velocity vector. The differential corrector targeting the Gateway's RIC could target points along this orbit's span by changing the launch epoch. Seven points were targeted with varying launch times. The launch epoch variable was tested by keeping the trip duration constant at 8400 seconds. To narrow in the optimal launch time, the epoch was adjusted manually. This incremental change allowed the Gateways RIC rates and fixed velocity vectors to be observed. The results of the seven locations and their calculated azimuth, elevation, and magnitude launch parameters are displayed in Table 4. Both the Gateway and payload's fixed velocity vectors in the X, Y, and Z directions were analyzed. Their magnitudes were calculated, and the difference between both absolute values is also presented in Table 4. Of the seven points targeted, trial 3 had the lowest difference magnitude (0.18052 km/s). The payload arrived at the space station on 6 Jan 2022 02:20:00.000 with an initial launch velocity of 2262.56 m/s.

D. LAUNCH DURATION

With a new target position selected, the next step was to find the optimal trip duration. The differential corrector used the stopping condition duration trip value as a control parameter. The perturbation was set to 0.1 seconds, and the max step was initially set to 60 seconds. The result constraints were still set to radial, in-track, and cross-track, and their tolerance was set to 0.0001 km. This scenario was run for five iterations, as seen in Table 5. The target sequence calculated values were inputted into the mission control sequence for each iteration and run again with a new smaller max step. Of the five trials, the third trial, with a 10-second max step, resulted in the smallest difference in magnitude of the terminal velocity with 0.018303 km/s. Of all the points analyzed on this model, this was the lowest achieved terminal velocity magnitude. This was achieved with launch specifications: azimuth of -134.427°, elevation of 59.1575°, and launch velocity of 2308.42 km/s. The RIC rates for both spacecraft are also listed in Table 6. As the trip duration grew beyond 21,500 seconds, the Gateways' orbit's slope grew larger, meaning the payload approach became more perpendicular to its target, increasing the difference in magnitude.

Table 4. Range of Launch Epochs Between Lunar Equatorial Plane at Apolune

	Epoch	TOF (s)	Azimuth (deg)	Elevation (deg)	Magnitude (m/s)	Radial Rate (km/s)	In-Track Rate (km/s)	Cross-Track Rate (km/)	Gateway V MAG (km/s)	Payload V MAG (km/s)	Difference in MAG (km/s)
1	5 Jan 2022 21:30:30.000	8400.0	-48.8355	12.2705	1957.740	-0.96788	-1.84278	-0.42061	23.53258	25.09547	1.56290
2	5 Jan 2022 22:56:00.000	8400.0	-130.890	33.4581	2090.680	-0.10583	-1.18697	0.90655	24.08569	25.23618	1.15050
3	6 Jan 2022 00:00:00.000	8400.0	-132.017	38.6291	2262.560	0.09394	0.20758	-1.16135	24.41124	24.59177	0.18052
4	6 Jan 2022 01:00:00.000	8400.0	-132.537	41.9297	2439.250	-0.01573	0.34284	0.70282	24.59272	24.19169	0.40102
5	6 Jan 2022 02:00:00.000	8400.0	-132.846	44.5826	2621.220	0.03690	0.78981	0.48684	24.72357	23.89837	0.82520
6	6 Jan 2022 03:00:00.000	8400.0	-133.04	46.837	2804.140	0.09203	1.14421	0.25697	24.82891	23.67062	1.15830
7	7 Jan 2022 03:00:00.000	8400.0	-130.74	68.1262	6200.170	1.52064	3.15696	-4.22225	26.4666	22.86316	3.60342

Table 5. Results of Differential Corrector Targeting Gateway RIC and Trip Duration of Trial 3

TOF (s)	Max Step	Azimuth (deg)	Elevation (deg)	Magnitude (m/s)	Radial Rate (km/s)	In-Track Rate (km/s)	Cross-Track Rate (km/s)	Gateway V MAG (km/s)	Payload V MAG (km/s)	Difference in MAG (km/s)
8400.0	60 sec	-132.017	38.6291	2262.56	0.093935	0.207584	-1.161353	24.411244	24.591768	0.180524
14929.8	30 sec	-133.451	52.5578	2289.42	-0.038139	-0.076378	0.575022	24.701620	24.732668	0.031048
21465.7	10 sec	-134.427	59.1575	2308.42	-0.025021	-0.005496	0.438341	24.887445	24.869143	0.018303
28003.4	1 sec	-135.208	63.2139	2319.94	-0.016656	0.02934	0.354992	25.037132	24.997971	0.039161
34541.8	0.1 sec	-135.000	66.3752	2321.54	-0.01639	0.048521	0.298982	25.171195	25.122152	0.049043

Table 6. RIC Rates for the Gateway and Payload at 6 Jan 2022 07:58:15.630

TOF (s)	Gateway RIC Rates (km/s)				Payload RIC Rates (km/s)			
	Vx	Vy	Vz	V MAG	Vx	Vy	Vz	V MAG
21465.7	14.28492	20.37915	-0.12859	24.88745	14.1939	20.41858	0.2992	24.86914

E. TARGETING GATEWAY RIC FOR ZERO RELATIVE VELOCITY

During this investigation, the smallest difference in the relative magnitude of velocity between the Gateway and the payload, found during the first and second orbits of the Gateway, was the space station's position on 6 Jan 2022 07:58:15.630. At this point, the difference in velocity observed was 18.303 m/s. This position was evaluated using the differential corrector to determine if the radial, in-track, and cross-track rates could be targeted by the payload to achieve our research objectives. Doing so forced the model to attempt to calculate a time and position in which the payload could be launched from the Moon and intercept the Gateway at the same position and a rate slow enough to avoid damage to the space station. To attempt this, the three new rates were coded as dependent variables into the differential corrector as results, seen in Figure 24. The Moon was selected as the central body, and the specified reference was set to the Gateway for each of the three rates.

Several strategies were deployed to get the rates to converge to zero. The goal was to designate a rate of 0.1 m/s for each of the rates to represent the payload matching the target rate on all axes. However, this needed to be walked in, and the first attempt was to target one of the rates. The first target was the radial rate, which was already the closest value to zero. The X, Y, Z cartesian thrust axes were used as control parameters and were set to 1 km at first to widen the search area and better calibrate the best guess to narrow in results. Various combinations of applying independent variables and dependent variables to be calculated by the model were attempted. Minimum tolerances of 1 km for the position and 0.1 m/s were selected for the rates. Knowing that the payload does not originate in the same orbit as the space station, we understand that the payload cannot achieve the same final position and velocity without a terminal maneuver. Instead, we targeted a RIC rate of

0.1 m/s, which would be an arrival rate slow enough not to damage the space station upon rendezvous. These parameters were inputted into the model, and no converged solution was found after hundreds of iterations.

Other attempts were made targeting two of the three rates in pairs, all three rates simultaneously, and with or without the epoch and duration selected as independent variables. None of these attempts resulted in a convergence. A third approach was to include the range rate as a dependent variable. This targeted the rate at which the range between the two objects converged. However, this also failed to result in a convergence in which any of the targeted RIC rates reached zero, while the RIC values also reached zero.

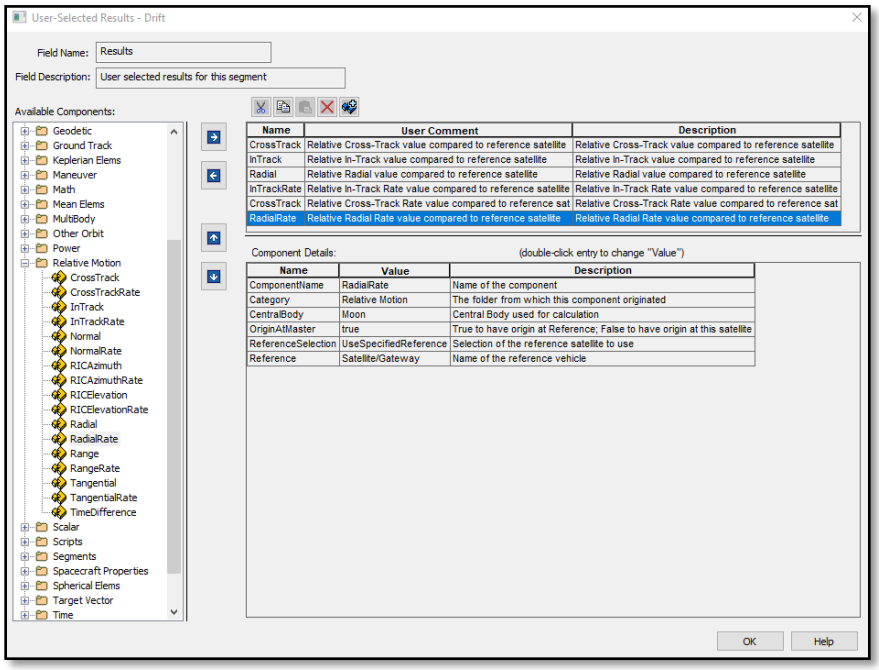

Figure 24. Adding Rates as Results Within the Propagate Segment

F. OTHER SCENARIOS TESTED

Once a minimum velocity magnitude was calculated, two other scenarios were tested. In the first scenario, an attempt was made to intercept the NRHO with two consecutive launches using the same thrust vectors, with variable launch epoch and trip

duration. In the second scenario, the launch epoch was targeted as a variable to show how the launch variables changed over a set amount of time.

1. Scenario 1

One consideration when postulating the practicality of using an EML on the Moon is the launcher's ability to launch several payloads in a short amount of time. Ideally, the launcher could be fired from a fixed launch direction, angle, and varying launch velocities to reduce the launch process's complexity and overall cost (I. McNab, email to author, January 8, 2021). This concept was tested using the STK model, where the differential corrector was used to target various combinations of launch variables at a lunch increment of one per hour. The scenario was set to 6 Jan 2022 with an initial launch time of 00:58:08.066, which is the optimal launch time previously calculated. In addition, the launch epoch was set to one hour in the future, the sequence only targeted trip duration, and three launch variables: azimuth, elevation, and magnitude, were fixed. When the target sequence was run for 500 iterations, it did not converge.

When the sequence does not converge, this means that no solution could be found where this launch resulted in a rendezvous with the Gateway on its trajectory. The scenario was rerun with the same launch epoch. This time, only the launch azimuth and elevation were fixed, with the launch magnitude and trip duration set as control parameters. Again, after 500 iterations, the payload did not intercept the Gateway. Only the elevation was a fixed constraint on a third attempt, while azimuth, magnitude, and trip duration were selected as control parameters. This time, the scenario converged, and the model calculated new results for the three control parameters. These conditions were run twice more at an interval of once per hour. Each time the scenario converged and new parameters were calculated. The results of this scenario are seen in Table 7. When the elevation was fixed, the azimuth changed by 0.30° per hour. The magnitude also changed by 4.42 m/s in the first hour, 4.49 m/s in the second hour, and 5.51 m/s in the third hour.

Table 7. Scenario 1 Launch Parameters

Converged	Launch Epoch	Azimuth (deg)	Elevation (deg)	Magnitude (m/s)	Trip Duration (s)
Yes	00:58:08.066	-138.83	74.5526	2348.72	73539.2
No	01:58:08.066	-138.83*	74.5526*	2348.72	-
No	01:58:08.066	-138.83*	74.5526*	2348.72	-
Yes	01:58:08.066	-138.53	74.5526*	2353.14	71381.9
Yes	02:58:08.066	-138.233	74.5526*	2358.08	69280.8
Yes	03:58:08.066	-137.94	74.5526*	2363.59	67235.4

*Variable held constant

2. Scenario 2

Knowing that the launch parameters change over time as the Gateway traverses its orbital path, an investigation was done into how quickly the launch parameters would change over several minutes. In scenario two, azimuth, elevation, magnitude, and trip duration were used as control parameters in the target sequence. Once again, starting with the optimum launch conditions on 6 Jan 2022, the launch epoch was incremented in the order of seconds to determine how quickly the launch variables strayed from the first result. The results of this scenario are seen in Table 8. In twenty minutes, the azimuth requirement changes by 0.052°, elevation changes 0.09°, and the magnitude of the velocity changes by 1.44 m/s.

Table 8. Scenario 2 Launch Parameters

Epoch	Time of Intercept	Time of Flight (s)	Azimuth (deg)	Elevation (deg)	Magnitude (m/s)
00:58:08.066	21:23:47.268	73539.2	-138.83	74.5526	2348.72
00:58:18.066	21:24:05.228	73537.3	-138.829	74.5532	2348.73
00:58:38.066	21:24:15.125	73537.1	-138.828	74.5546	2348.76
00:58:48.066	21:24:25.022	73537.0	-138.828	74.5554	2348.77
00:58:58.066	21:24:34.920	73536.9	-138.827	74.5561	2348.78
00:59:08.066	21:24:44.817	73536.8	-138.827	74.5569	2348.79
01:08:03.960	21:33:35.230	73531.3	-138.804	74.5963	2349.44
01:18:03.960	21:43:29.163	73525.2	-138.778	74.6403	2350.16

G. ACHIEVING RENDEZVOUS WITH THRUSTERS

In the final scenario, two variants of thruster engines were modeled on the payload. For both scenarios, the payload was launched on 6 Jan 2022 01:18:03.960 UTCG, and after

a trip duration of 115,698 seconds, and the payload reached a point within five kilometers of the Gateway. At this target location, the payload's engine performed a single maneuver targeting the Gateway. This maneuver was modeled using a second targeting sequence. The payload was redirected towards the space station, arriving at a velocity within 0.0001 km/s of the Gateway's relative velocity. The mission control sequence used in this model is seen in Figure 25.

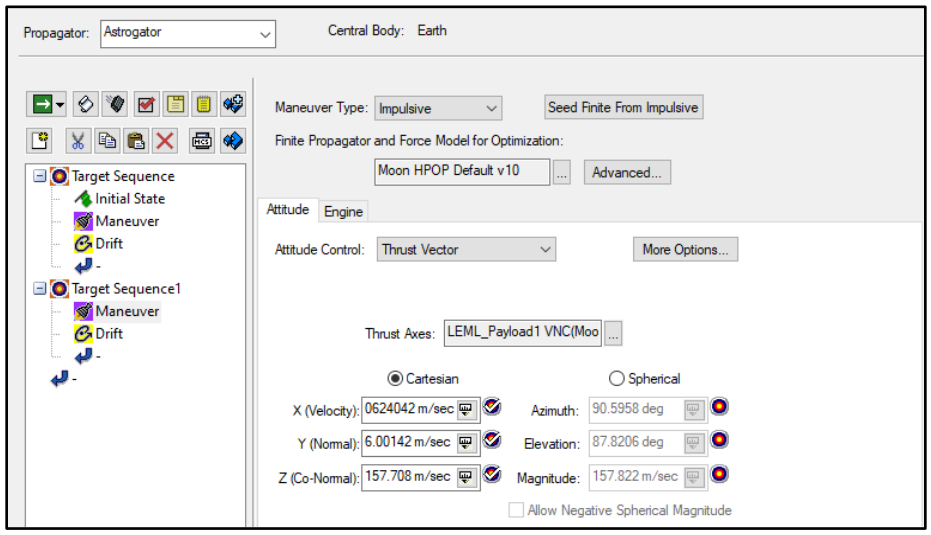

Figure 25. Second Target Sequence added to the Mission Control Sequence

The first engine type that was modeled was a chemical engine, and the results of intercept are seen in Table 9. The engine parameters coded into the model included 500 Newtons (N) of thrust and an I_{SP} of 300 seconds. When the two differential correctors were run, both converged, meeting the Gateways with a RIC of 0 km, with a 0.0001 km tolerance, and RIC rates of 0 km/s, with a 0.0001 km tolerance as seen in Figure 26. The 3D Graphics window is also seen in Figure 27. The maneuver took 307.5 seconds, and with a 70 kg payload, the maneuver would take 35.97 N of thrust using a chemical propellant engine.

Table 9. The Difference in Fixed Velocity at Intercept with Chemical Engine

	Vx (km/s)	Vy (km/s)	Vz (km/s)	V MAG (km/s)
Gateway Fixed Velocity	3.796332	27.666084	0.298025	27.926925
Payload Fixed Velocity	3.796302	27.666053	0.29809	27.926891
Difference (km/s)	-0.0000300	-0.0000310	0.0000650	-3.40949E-05

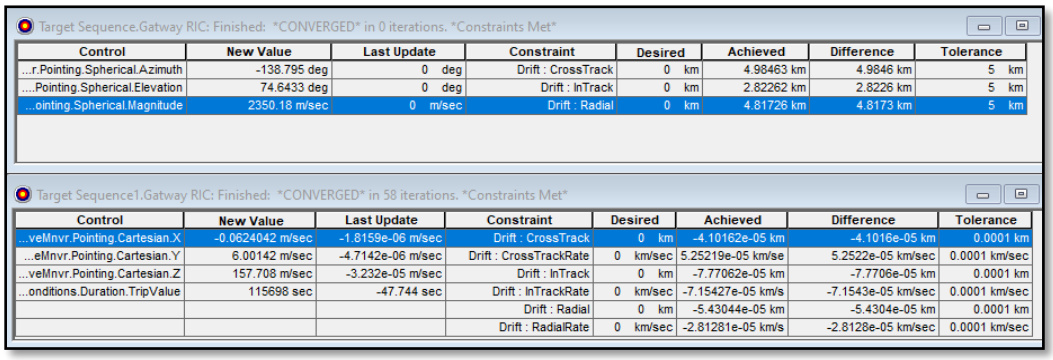

Figure 26. Target Sequence Results for a Chemical Engine

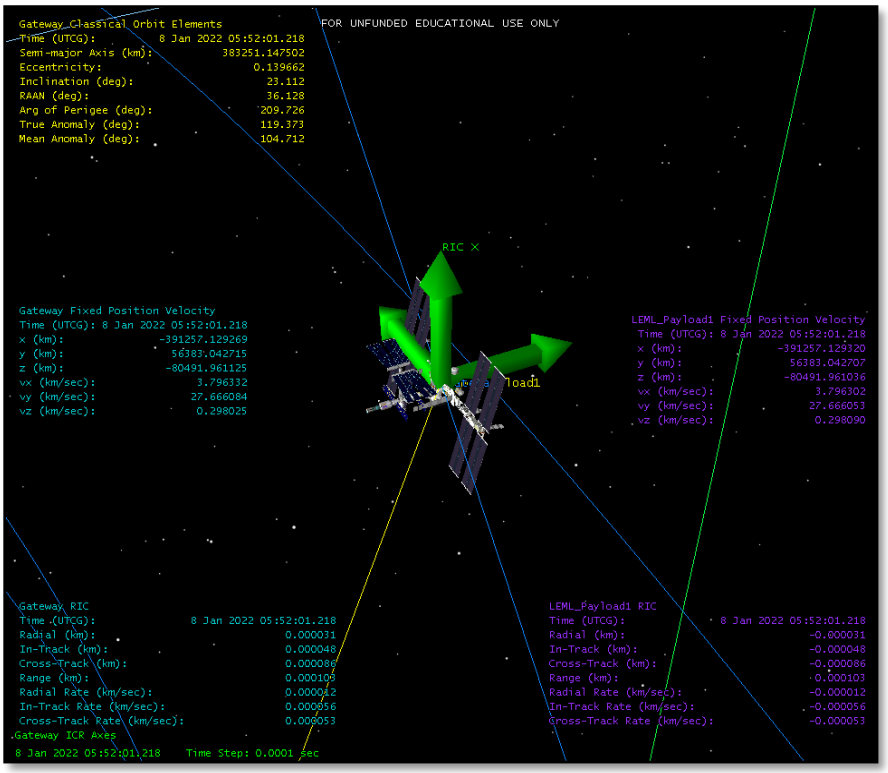

Figure 27. 3D Graphics at the Point of Intercept Using a Chemical Engine

The second engine type that was modeled was a cold gas engine. This scenario also converged on both target sequences, and the results of the rendezvous are seen in Table 10. The engine parameters coded in the model were 3.5 Newtons (N) of thrust and an I_{SP} of 70 seconds. This I_{SP} could be achieved with a nitrogen gas thruster. The RIC and RIC rate tolerances were set the same as the chemical scenario, as displayed in Figure 28. The 3D Graphics window in Figure 29 also shows the rendezvous point, along with the RIC values for both the Gateway and the payload. The maneuver took 2,818.8 seconds, and with a 70 kg payload, the maneuver would take 3.917 N of thrust.

Table 10. The Difference in Fixed Velocity at Intercept with Cold Gas Engine

	Vx (km/s)	Vy (km/s)	Vz (km/s)	V MAG (km/s)
Gateway Fixed Velocity	3.291450	27.726835	0.29668	27.923102
Payload Fixed Velocity	3.291421	27.726804	0.297732	27.923069
Difference (km/s)	-0.0000290	-0.0000310	0.0000640	-3.35182E-05

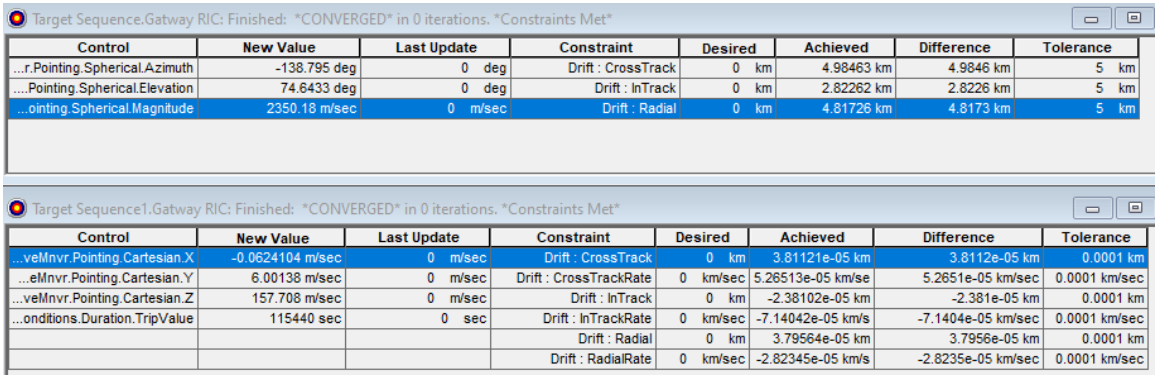

Figure 28. Target Sequence Results for a Cold Gas Engine

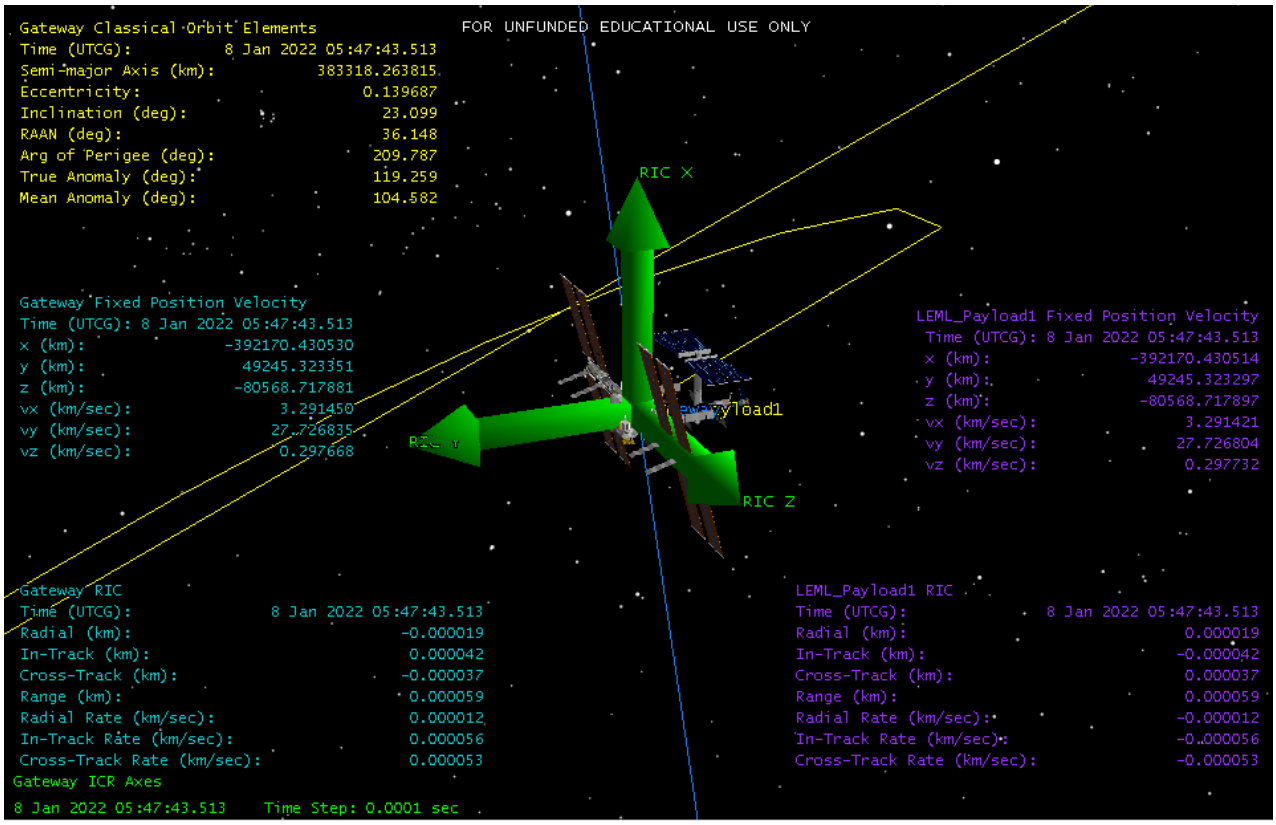

Figure 29. 3D Graphics at the Point of Intercept Using a Cold Gas Engine

THIS PAGE INTENTIONALLY LEFT BLANK

V. CONCLUSION AND RECOMMENDATIONS

The results produced by the model allowed the researcher to investigate the feasibility of intercepting the Gateway with a LEML payload at a rate near relative rest. These conclusions are presented, along with recommendations for alternative means of achieving rendezvous and ideas for this research model's future applications.

A. CONCLUSIONS

The problem identified for this research can be split into two parts. The first asks if a self-contained payload containing either raw ice or LH_2 can feasibly intercept the Gateway's orbit. The second part of the problem statement is whether the payload can match the space station's position and velocity. Results were reviewed in the form of tables and 3D graphics. It was concluded that though it is possible to intercept the Gateway at any point along the NRHO from a polar launch, it is impossible to intercept it at a relative velocity matching that of the Gateway using just the initial launch velocity.

1. Support for the Hypothesis

This research's hypothesis stated that the payload would reach the Gateway at several points along the spacecraft's trajectory when launched with a velocity less than 2.8 km/s. The student postulated that the payload would not achieve a terminal velocity near rest and that further modifications to the payload to account for additional flight hardware would be required. The results of this study present evidence to support this hypothesis.

The model was produced to replicate the launch parameters. The Gateway's irregular orbit was used to show that the Gateway could be targeted at all four of the postulated points. With the varying launch, parameters the payload could reach any point along the space station's orbit. The largest recorded launch velocity was 6.20 km/s, though this was when the trip duration was fixed at 8200 seconds to target one of the farthest points on the orbital path. With variable trip duration, launch epoch, and other launch parameters, the same location was routinely reached with a launch velocity between 2.289 and 2.486 km/s, well under the hypothesized 2.8 km/s.

2. Optimal Launch Parameters

The lowest relative velocity between the two objects was 18.303 m/s, and this was only achieved once along the NRHO with the launch parameters seen in Table 11. The azimuth, elevation, and magnitude required to achieve this interception are all reasonable within the proposed LEML specifications' constraints postulated for this mission. It is important to note that during the investigation into this optimal result, the model calculated this result by walking into a solution by adjusting the max step or variation between each calculation for the trip duration. The best result was achieved with a max step of 10 seconds. However, when the max step was reduced to 1 second and 0.1 seconds, respectively, the result was a higher change in magnitude of the relative velocity. In theory, as the calculation becomes more precise, a better, more exact result should have been calculated. The results show that the time of flight between 14929.8 and 28003.4 seconds provided the smallest difference in magnitude between the two objects. Further investigation into replicating this result may be needed to explain why the results did not improve as the max step decreased. This was not investigated further during this study.

However, the 18.303 m/s result that was analyzed is a relative speed that surpasses optimal rendezvous conditions by 13 to 17 m/s. Optimally, a rendezvous would need to take place at an approximate velocity of one to five m/s to avoid damage to the space station or the Gateway's ability to maintain its current orbit. Alternative methods will need to be further explored to achieve a more manageable relative magnitude of both objects' velocity. The exploration into the use of terminal guidance thrusters or an alternative, space based, catching method is required.

Table 11. Optimal Position

Launch Epoch (UTGC)	TOF (s)	Azimuth (deg)	Elevation (deg)	Magnitude (m/s)	Δ V MAG (km/s)
6 Jan 2022 00:00:00.000	21465.7	-132.017	38.6291	2262.560	0.018303

3. Conclusions from Other Launch Scenarios

Conclusions were also drawn from the other two scenarios tested by the model. The results for both launch scenarios tested yielded launch conditions that are technically feasible for the railgun. These results impact future decisions for how the launcher may target the space station and, therefore, the launcher's specifications.

a. Scenario 1

The results presented in scenario one demonstrated that an hourly launch is possible when the elevation remains constant, and the azimuth and magnitude of launch remain variable. The magnitude and azimuth need to be incrementally changed within the hour for a subsequent launch to be successful and be able to intercept with the Gateway again. The results seen from the analysis of the first four points along the NRHO suggest that an hour launch scheme can only be accomplished as the space station traverses from the lunar equator to the orbit's apolune. The closer the stations got to the apolune, the more significant the deviation in results. At this point in the orbit, the flight path angle approaches zero. The angle of intercept between the two objects becomes more perpendicular, increasing the fixed velocity vectors' magnitude.

b. Scenario 2

Scenario two expands upon the conclusions found in scenario one. If the launcher aims to target the orbit's points with the lowest relative difference in velocity, the available launch window will be fleeting and only occur once every seven days. It is realistic to expect that the launcher will be required to launch several shots per minute over several minutes to reach the Gateway with sufficient material. The results from scenario 2 seem to show that this would be feasible within this time frame. When the values were incremented slowly, the change in launch parameters deviated by 0.001 in azimuth, 0.0006 in elevation, and 0.01 m/s in magnitude. Further analysis will be required once a final launch location and launcher specifications are determined. Still, these results demonstrate that launching several payloads within a short amount of time, an action current railgun technology can achieve, will be feasible when targeting the Gateway's orbit.

B. RECOMMENDATIONS

The research statement's subsidiary research questions involve the need for terminal guidance thrusters. This study's results clarify that a secondary means will be required to slow the payload down before intercepting its moving target. This model could not calculate a single launch configuration that would allow for an intersection at a rate difference below 18.303 m/s, which is significantly too fast to safely intercept an object within the NRHO. However, it could calculate a successful interception with a second maneuver using two different engine types. It is recommended that further research be conducted regarding the use of terminal guidance thrusters in the payload's design to achieve a terminal velocity matching the Gateway.

1. Thruster Parameters

Trajectory control, when required, utilizes a spacecraft's propulsion system to alter the magnitude and direction of the vehicle's vector. However, the payload being launched by the LEML inherently does not have its own propulsion system, and the addition of this capability will impact the payload's ability to transport material. Any additional trajectory control hardware will add extra weight and consume additional space within the packaging, both of which will reduce the amount of raw material that can be transported with each launch. Because the payload does not originate in the Gateway's orbit, we know that a second burn will be required for the payload to rendezvous with the Gateway and match the space station's position and velocity. One option for this burn would be a single, relatively short, duration burn of 157.82 m/s within five kms of the Gateway. Depending on the type of engine, this burn would be longer than a typical impulsive burn but relatively smaller than the payload's second coast which would last more than a day in duration. Having a small thrust requirement provides options regarding the type of engine used to achieve the new vector for intercept. Although, alternative catching methods would require even less ΔV.

Table 12. Required Maneuver by Payload Engine

Engine Type	Short Duration Maneuver Cartesian Coordinates				Burn Time (s)	Required Thrust (N)
	X (m/s)	Y (m/s)	Z (m/s)	MAG (m/s)		
Chemical	-0.0624042	6.00142	157.708	157.82216	307.50	35.970
Cold Gas	-0.0624104	6.00138	157.708	157.82216	2818.8	3.9176

Electromagnetic launchers add additional physical limitations on the payload that must be accounted for in the design. If we estimate a barrel length of 60 m and use a launch velocity of 2.26 km/s we can define the muzzle velocity (m/s) by:

$$v_{muz}^2 = 2as \,, \tag{5}$$

where:

a=Acceleration (m/s^2)
s= Barrel Length (m).

Using equation (5), the payload would accelerate at 42.6 km/s^2. At this acceleration, the estimated gun bore pressure would be 400 MPa. Any thrusters, fuel containment for the thrusters, and any avionics used to orientate the object during the burn needed in this scenario must survive launch. Other extraneous launch conditions would include vibration and shock. All these factors will put significant restrictions on the type of engine selected.

a. Engine Types

According to the Space Mission Engineering: New SMAD (2011), several types of rocket engines are used in space operations. These engine types, along with application and achievable I_{SP}, can be found in Table 13. In the industry, current propulsion options for trajectory control include cold gas, liquid (monopropellant, bipropellant, dual-mode, hybrid), and electric. Solid chemical motors are typically used for orbit circularization at apogee and perigee for orbital insertion (Wertz et al., 2011).

Table 13. Overview of Common Application for Different Propulsion Systems. Source: Wertz et al., (2011).

Propulsion System	Orbit Insertion		Orbit Maintenance & Maneuvering	Attitude Control	Typical Range of I_{SP} (Seconds)
	Perigee	Apogee			
Cold Gas			x	x	45-73
Solid	x	x			290-304
Liquid-Monopropellant			x	x	200-235
Liquid-Bipropellant	x	x	x	x	274-467
Electric		x		x	500-3000

When comparing the performance produced by each engine, there are several factors to consider when approaching the LEML payload problem set. The required low thrust and I_{SP} means that cold gas and liquid propellent are both viable options. These options are also supported by Figure 30, which shows the effective exhaust velocity verse the required thrust and how each of these engine types compares under these conditions as described by Sutton and Biblarz in their 2017 *Rocket Propulsion Elements* textbook. Three engine types were considered in this study. They include cold gas thrusters, liquid-monopropellant engines, and solid motors.

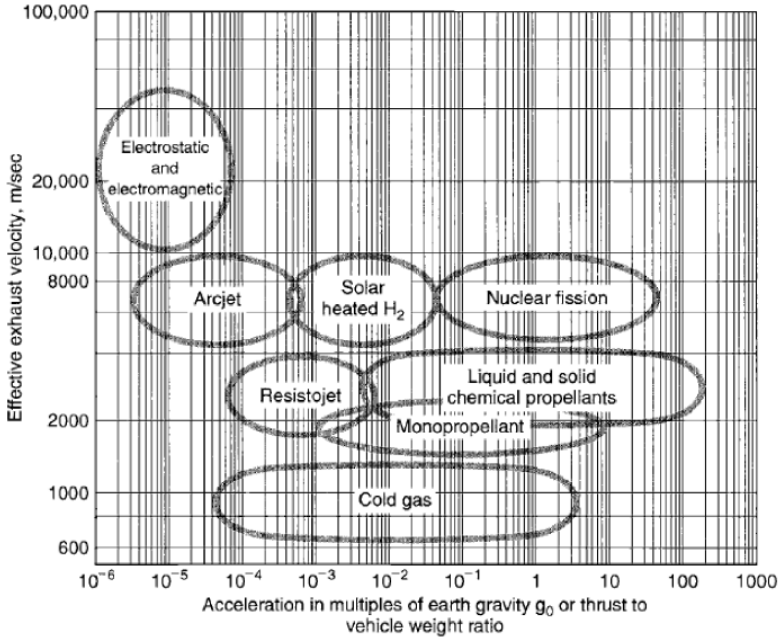

Figure 30. Exhaust Velocities as a Function of Typical Vehicle Accelerations. Source: Sutton and Biblarz, (2017).

(1) Cold Gas Thrusters

According to the New SMAD, cold gas thrusters do not require combustion to generate thrust. Instead, thrust is produced by expanding high-pressure gas through a converging-diverging nozzle. This gas is fed to the nozzles, orientated in three or more axes, from a pressurized tank filled with inert gas (Wertz et al., 2011). These thrusters have the lowest I_{SP} of all the engine types but are useful in missions that require small ΔV maneuvers, like in this scenario. A cold gas thruster used 5 km from the gateway intercept point would provide a sufficient thrust and exhaust velocity to meet the single burn needed for this maneuver.

The gasses commonly used by these thrusters are helium, nitrogen, and freon (Wertz et al., 2011). Experiments conducted by Apollo 17 and LCROSS have shown that the moon has traces of an atmosphere made up of helium and argon, along with traces of ammonia, methane, and carbon dioxide (Dunbar, 2013). Therefore, helium (I_{SP} of 165 s) and possibly ammonia (I_{SP} of 96 s) could be used as a source of the gas used in these thrusters (Wertz et al., 2011).

Described by Assad Anis in a paper published by *Remote Sensing - Advanced Techniques and Platforms* (2012), one concern using cold gas thrusters would be the total weight added to the payload. The thruster themselves are small and weigh 0.01-1 kg; however, additional space and mass must house the gas tanks. Helium gas would have a low molecular weight but also an increased tank volume. The high-pressure storage tank needed to house the gas would weigh more than other gas systems (Anis, 2012). The small particle size also leads to leaking issues which will also be a concern (Wertz et al., 2011).

Though not typically used due to safety and storage concerns, liquid hydrogen could be used as the propellant in a cold gas system. A specially designed system could, in theory, be developed to use the transported hydrogen to complete the maneuver required for this mission. Using the onboard fuel would reduce the space and mass requirement of an additional tank.

More importantly, the survivability of these thrusters remains a concern in including them in the payload design. Most testing on these devices is conducted to test the

operating pressure as the gas exits the tank through the valve and inlet. Some inlets tested by Vacco Industries in 2004 could survive up to 5400 psia. However, tests for pressure experienced on the system is not available (Vacco Industries, 2004). Vibration testing and thermal vacuum testing results can be found on systems flown. However, even these tests do not mimic the extreme conditions the system would experience during LEML launch (Harmann et al., 2016). Special housing and protections would be required to harden these pressurized tanks. The standard tank mounts and tabs used to keep the tanks tightly fitting into the payload would have to be explicitly tested for their ability to function after EML.

(2) Liquid monopropellant Engines

Liquid rocket engines are very versatile and can be employed at various points in a spacecraft's mission. Each of the different engine configurations—monopropellant, bipropellant, dual-mode, hybrid —has its advantages and disadvantages, as discussed in the *Space Mission Engineering: The New SMAD* (2011). For the sake of this scenario, however, simplicity, occupying space, and reducing weight remain the primary drivers in selection. Engines with more than one propellent type often provide higher I_{SP} and thrust. However, this scenario requires a relatively low thrust requirement. For these reasons, monopropellant was explored as the leading engine type for its simplicity and only requiring one storage tank.

Monopropellant systems decompose one propellent type exothermically when the liquid propellent passes over a catalytic bed (Harmann et al., 2016). This action heats the liquid, converting it into a high-pressure gas that, when expanded through a converging-diverging nozzle, generates thrust. These engines' expected I_{SP} range is 165–244 seconds and is typically used in operations that require a ΔV not exceeding 1000 m/s, making them a possible fit for this research scenario. These results are commonly achieved with a hydrazine propellant and iridium-coated aluminum oxide (Harmann et al., 2016).

Like the cold-gas thrusters, monopropellants still require a high-pressure tank that would need to maintain structural integrity during LEML. Launch conditions would need to be explicitly tested on the selected system to determine its function post-launch. Hydrazine is also not a chemical compound found on the Moon. Hydrazine would need to

be procured from Earth, adding to the complexity of using this system in the LEML payload.

(3) Solid Motors

Nottke and Bilby (1990) considered using a solid kick motor to insert their proposed LEML payload into a 100 km circular orbit to collect until retrieval is possible (p. 4). In this case, a single solid apogee burn to move the payload into a collection orbit makes sense. Solid rocket motors are the simplest of the available engines, in the sense that they do not have moving parts, apart from the nozzle, and have higher density fuel that requires less space to house (Harmann et al., 2016). The simplicity in their design means that these motors would have a high likelihood of surviving LEML launch stresses. The downside, however, is that once they are ignited, these motors are not turning off, requiring known total impulse for one specific maneuver (Harmann et al., 2016). If the mission were to intercept our target simultaneously once per orbit, this could be useful; however, the launch parameters are variable as the Gateway traverses its orbit, making the use of these rocket motors in our scenario not practical.

2. Commercial-Off-the-Shelf Thrusters

Finding a thruster system readily available on the commercial market that meets the launch specifications proved difficult. Without access to testing conditions posed on available hardware, it is difficult to determine whether these thrusters would survive EML conditions. Even commercially available hardware would likely require modification to meet the specific requirements of this launch scenario. Of specific concern are the pressurized tanks and how they would fair under the extreme bore pressure and launch shock.

Several cold gas and monopropellant thrusters on the market would have the I_{SP} and thrust required of this single corrective maneuver. Two cold gas thrusters investigated include the Moog triad thruster and the Vacco cold gas triad thruster (Crone, 2017 & Vacco, 2004). Both are nitrogen-based systems, which is not ideal for this scenario, but both thrusters have a three-axis manifold block, can achieve an I_{SP} of 73 seconds, and would be capable of providing the needed 3.9 N of thrust (Crone, 2017).

The liquid monopropellant engines on the market capable of producing 35.97 N of the thrust are larger in size and weight when compared to the cold gas thrusters. Most of the smaller variants go up to 20–22N of thrust before jumping to a larger variant upwards of 100s of Newtons. One variant that may be worth exploring further would be the Aerojet MR-107N, with a thrust of 109–296N and an I_{SP} of 229–232. This thruster is smaller, weighing only 0.74 kg dry, and- would be able to complete the maneuver (Harmann et al., 2016).

C. FUTURE RESEARCH

The model created to explore the research statement and hypothesis for this study could easily be modified to explore other specific questions regarding the use of LEML on the Moon's surface. This model was created to determine the feasibility of intercepting the NRHO from a single location on the Moon. Further research should be conducted using the STK's Analysis Workbench in conjunction with the created model to determine if reducing the relative velocity further is possible. Future research could also explore variables not investigated by this study, including launch location, other intercept target locations, alternatives to payload engines, and the payload's specifications.

One tool that was not leveraged during this study was the use of STK's Analysis Workbench. This application expands the underlying computational capabilities of STK. It allows the user to generate custom components regarding vector geometry, time, calculations, and spatial analysis, all of which could be useful in further analysis for this research topic (STK, 2021c). Leveraging this tool's power to code time and vector components could provide further analysis that STK's astrogator was not capable of doing on its own. This tool could be used to verify the optimal solution found that resulted in the approximate 18 m/s rendezvous and find alternative rendezvous locations along the space station's orbit that can intercept the gateway at a terminal velocity between one and five m/s, a speed considered slow enough to be caught by the station. One scenario that was also not tested using this model was conducting a reverse launch sequence from the Gateway to the launch location. Doing this sequence in reverse from how it is currently

modeled could provide an optimal initial launch condition. The analysis Workbench could be used to help run this calculation in future testing.

Investigating other launch positions would also be a way to add to the research presented by this thesis. Positioning the launcher at other latitudes on the Moon's surface would be the first place to start. The results of the model showed that in order to reach the apolune or point along the orbit in which the space station is the slowest, a near-vertical launcher was required at the south pole. A vertical launch would likely require a buried configuration for the LEML. However, if the launch location were moved away from the center of the pole, the natural curvature of the Moon would reduce the required azimuth for the same target. Positions around the -30° lunar latitude could be one location to investigate. Positioning the launcher on the equator could also be another option. Launching at this location benefits from the Moon's rotation. The ability to launch at an elevation near zero while oriented parallel to the NRHO could also provide circumstances where the relative velocity difference is significantly reduced. With more research emerging that water and ice are locked inside the lunar regolith at various latitudes on the sunlit side of the Moon, like in the SOFIA study published by Honniball et al. in 2020, there may be more freedom regarding where the launcher could be placed. The built STK scenario could easily model this by amending the initial state within the target sequence to reflect the new launch location and running the differential corrector to target the same locations along the Gateway's orbit.

Another option for further research would be to place a fuel depot in a more stable location, such as L_1 or L_2. Though these locations would require station keeping, investigating these targets may prove more accessible from the lunar south pole. The problem of getting the fuel from this location to the space station or future missions requiring the propellant would need to be investigated further. The model created for this thesis was not explicitly designed to include launches to orbits or Lagrange points other than NASA's selected NRHO. However, STK and the Analysis Tool Kit can target these other locations surrounding the Moon.

This paper investigated a possible solution for using an engine on the payload to complete rendezvous with the space station. A second burn will be required for the payload

to match the space station's relative position and velocity and this research demonstrates that the required terminal maneuver would require 18.3 m/s at the point of rendezvous or 157.82 m/s within five km of the space station. However, other options may exist, outside of on-board thrusters, that could aid in accomplishing rendezvous. One possible solution may be a catch mechanism co-located with the Gateway that can receive the payload when its velocity difference is approximately 18 m/s from the space station. If a net were used with its own thruster capability, the payloads could be caught by the space station without the need to slow the package down further with a second burn. Thrusters and fuel required to transfer the payload's energy and maintain the catch device in the required orbit with the Gateway would be located on the catching device itself and could be reused with each payload launch. The payload launched from the rail gun would then require a much smaller engine and fuel load to accomplish an exact required Δ V for rendezvous. The combination of these methods would save space and weight and allow for more propellent materials to be launched from the Moon. This type of solution would increase the complexity of the problem but could result in the ability to transport more raw materials into space. Further investigation into space-based devices should be considered in future research.

The final item that should be considered in future research would be the payload parameters. The payload used in this research was a hypothetical 70 kg payload. Its shape, contents, mass, and other parameters were not studied or investigated during this research. Once further studies have been conducted regarding what is feasible for this package, these parameters will also need to be included in future models. The addition of thrusters or a kick motor for a final interception with the payload's target will also require significant modifications to the payload design. The engine selected will require extensive environmental testing outside the usual vibration and pressure testing to ensure the launch's components.

LIST OF REFERENCES

Anand, M., Crawford, I. A., Balat-Pichelin, M., Abanades, S., van Westrenen, W., Pe´raudeau, G., . . . Seboldt, W. (2012). A brief review of chemical and mineralogical resources on the Moon and. *Planetary and Space Science*, 42–48. https://doi.org/10.1016/j.pss.2012.08.012

Anis, A. (2012). Cold gas propulsion system - an ideal choice for remote sensing small satellites. *Remote Sensing - Advanced Techniques and Platforms*, 447–462.

Berger, E. (2019, July 31). *NASA agrees to work with SpaceX on orbital refueling technology.* ars Technica. https://arstechnica.com/science/2019/07/nasa-agrees-to-work-with-spacex-on-orbital-refueling-technology/

Beemer, H. D. & Worrells D. S. (2017) Conducting rock mass rating for tunnel construction on Mars. *Acta Astronautica, 139,* 176–180. https://doi.org/10.1016/j.actaastro.2017.07.003

Chato, D. (2005). *Low gravity issues of deep space refueling.* NTRS.

Clark, A. C. (1950). Electromagnetic Launching as a Major Contribution to Space-Flight. *Journal of the British Interplanetary Society,* 9(6), 261–267.

Crone, C. (2017). *Cold gas thruster triad.* MOOG Space and Defense Group. https://satcatalog.com/datasheet/MOOG%20-%2050-820%20Triad.pdf

Dunbar, B. (2013, April 12). *Is there an atmosphere on the Moon?* NASA. https://www.nasa.gov/mission_pages/LADEE/news/lunar-atmosphere.html

Fields, S. A., Weathers, H. M., Cox, R. M., & Shotts, R. Q. (1967). *Problems and techniques of lunar surface mining.* NTRS.

Green, R. D., & Kleinhenz, J. (2019). In-situ resource utilization (ISRU). *Proceedings of the ACS National Meeting& Exposition 257*, 1–41. https://ntrs.nasa.gov/api/citations/20190025283/downloads/20190025283.pdf

Harmann, H-P., Rombach, T., & Dartsch, H. (2016). Cold gas thruster qualification for FORMOSAT 5. *Advanced Space Technologies.* https://satcatalog.com/datasheet/Advanced%20Space%20Technologies%20-%20CGT.pdf

Honniball, C. I., Lucey, P. G., Li, S., Shenoy, S., Orlando, T. M., Hibbitts, C. A., . . . Farrell, W. M. (2020). Molecular water detected on the sunlit Moon by SOFIA. *Nature Astronomy*. https://doi.org/10.1038/s41550-020-01222-x

Jacobs, W. A., & Montenegro, J. (2000). *Magnetic launch assist: NASA's vision for the future.* NTRS.

Jones, H. (2018). *The recent large reduction in space launch cost.* [Paper presentation]. 48th International Conference on Environmental Systems. Albuquerque, NM, United States.

Lee, D. E. (2019). *White Paper: Gateway destination orbit model: a continuous 15 year NRHO reference trajectory*. (Report No. JSC-E-DAA-TN72594). NASA Johnson Space Center. https://ntrs.nasa.gov/api/citations/20190030294/downloads/20190030294.pdf

McNab, I. R. (2013). Electromagnetic augmentation can reduce space launch costs. *IEEE Transactions on Plasma Science*, 41(5), 295–304. 10.1109/TPS.2013.2241452

McNab, I. R., & McGlasson, B. T. (2020*). Introduction to railguns (Distro-D).* [Lecture]. Naval Postgraduate School, Monterey, CA.

National Aeronautics and Space Administration. (2020a). *NASA's lunar exploration program overview*. https://www.nasa.gov/sites/default/files/atoms/files/artemis_plan-20200921.pdf

National Aeronautics and Space Administration. (2020b). The *Artemis Accords.* https://www.nasa.gov/specials/artemis-accords/img/Artemis-Accords-signed-13Oct2020.pdf

Newman, C. P., Davis, D. C., Whitley, R. J., Guinn, J. R., & Ryne, M. S. (2018). *stationkeeping, orbit determination, and attitude control for spacecraft in near rectilinear halo orbits.* [Paper presentation] AAS/AIAA Astrodynamics Specialist Conference. Snowbird, UT, United States.

Noneman, S. (2007). *Is there water on the Moon? NASA's LCROSS mission.* [Lecture] The University of Cincinnati Department of Aerospace Engineering and Engineering Mechanics Graduate Seminar, Cincinnati, OH, United States. https://ntrs.nasa.gov/api/citations/20080015767/downloads/20080015767.pdf

Nottke, N., & Bilby, C. (1990). *A superconducting quenchgun for delivering lunar derived oxygen to lunar orbit.* NTRS.

Office of the Press Secretary (2004, January 14). *President Bush announces new vision for space exploration program*. NASA. https://history.nasa.gov/Bush%20SEP.htm

Potter, S. & Warner, C. (2020, October 13). NASA, international partners advance cooperation with first signings of Artemis accords. NASA. https://www.nasa.gov/press-release/nasa-international-partners-advance-cooperation-with-first-signings-of-artemis-accords

Sellers, J. J., Astore, W. J., Giffen, R. B., & Larson, W. J. (2000). *Understanding space: An introduction to astronautics* (2nd ed.) (1215906998 905420816 D. H. Kirkpatrick, Ed.). New York, NY: McGraw-Hill.

Semenov, B. (2020, December 20). *The SPICE concept.* JPL. https://naif.jpl.nasa.gov/naif/spiceconcept.html

Siegfried, W. H. (2000). Use of propellant from the Moon in human exploration and development of space. *Acta Astronautica*, 47, 365–375. https://doi.org/10.1016/S0094-5765(00)00078-3

Snow, W. R., & Kolm, H. H. (1992). *Electromagnetic launch of lunar material.* NTRS.

Starr, S. (2010). *eLaunch hypersonics: an advanced launch system.* NTRS.

Stewart, M. C. (2016). Comparison of two railgun power supply architectures to quantify the energy dissipated after the projectile leaves the railgun. NPS Archive: Calhoun, Master's thesis, Naval Postgraduate School. https://calhoun.nps.edu/handle/10945/49392

Sutton G. P., & Biblarz O. (2017). *Rocket propulsion elements.* (9th ed.). John Wiley & Son.

Systems Tool Kit. (2021a, February 1). *High-precision orbit propagator (HPOP).* https://help.agi.com/stk/index.htm#hpop/hpop.htm?Highlight=HPOP%20propagator

Systems Tool Kit. (2021b, February 1). *Technical overview of central body reference Frames (Coordinate Systems).* https://help.agi.com/stk/index.htm#stk/referenceFramesCentralBodies.htm?Highlight=Reference%20frame%20J2000

Systems Tool Kit. (2021c, February 18). *STK analysis workbench.* https://www.agi.com/products/stk-systems-bundle/stk-analysis-workbench

Vacco Industries (2004). *Space products cold gas thrusters.* https://www.vacco.com/images/uploads/pdfs/cold_gas_thrusters.pdf

Wertz, J. R., Everett D. F., & Puschell J. J. (2011). *Space Mission Engineering: The New SMAD.* Microcosm Press.

Whitley, R., Lee, D., Acton, C., & Knopf, W. (2018, July 18). Sample deep space Gateway orbit. JPL. https://naif.jpl.nasa.gov/pub/naif/misc/More_Projects/DSG/

Williams, D. R. (2020) *Moon fact sheet*. NASA. https://nssdc.gsfc.nasa.gov/planetary/factsheet/moonfact.html

Wright, M. R., Kuznetsov, S. B., & Klosel, K. J. (2011). A lunar electromagnetic launch system. *IEEE Transactions on Plasma Science*, 521–528. https://doi.org10.1109/TPS.2010.2089066

Zimovan, E. M., Howell, K. C., & Davis, D. C. (2017). *Near rectilinear halo orbits and their application in cis-lunar space.* [Paper presentation]. 3rd IAA Conference on Dynamics and Controls of Space Systems, San Diego, CA, United States.

INITIAL DISTRIBUTION LIST

1. Defense Technical Information Center
   Ft. Belvoir, Virginia

2. Dudley Knox Library
   Naval Postgraduate School
   Monterey, California